Original paper

GEOPHYSICS FOR GEOTHERMAL EXPLORATION. DIRECTIONAL-DERIVATIVES-BASED COMPUTATIONAL FILTERS APPLIED TO GEOMAGNETIC DATA AT LAKE CUITZEO, MEXICO

Alberto Mazzoldi[1,2*], Victor Hugo Garduño-Monroy[1†], Joaquín José Gómez Cortes[1] and Jorge Alejandro Guevara Alday[1]

Received: July 30, 2019; accepted: March 2, 2020; published online: April 1, 2020

RESUMEN

Para el desarrollo de un campo geotérmico, el conocimiento de la distribución de fracturas, la hidrología y la evolución tectónica del sitio a través de la caracterización estructural del sistema natural es un requisito previo a la perforación de pozos exploratorios. Fallas y fracturas representan vías preferenciales por el flujo de fluidos en el subsuelo y pueden ser detectadas mediante investigaciones geológicas en la superficie y geofísicas en el subsuelo. Una anomalía magnética positiva y de forma sub-circular en planta se encuentra en el medio del lago Cuitzeo, México. A través de un levantamiento geomagnético dentro y alrededor del área que comprende la anomalía tratamos caracterizar el reservorio geotérmico que, al sur del lago, está notificado por manifestaciones hidrotermales. Utilizando filtros computacionales basados sobre el uso de operaciones con las derivadas de valores de campo a los datos magnéticos grabados, hemos puesto en luz algunas de las estructuras que influencian la circulación de los fluidos en el sistema geotermal. Nuestra atención se focalizó sobre fallas ~N-S and E-W, pertenecientes respectivamente a la tectónica Básin & Range (B&R) y a la del Cinturón Volcánico Mexicano (CVM). Según nuestra interpretación, la interacción de dos o mas estructuras de diferentes orígenes (B&R y CVM), además del entorno geodinámico específico (subducción de zona de fracturas), facilitó el surgimiento de cuerpos magmáticos básicos del profundo que, bloqueados por la capa argilosa de sedimentación lacustre del Cuitzeo, dieron lugar, enfriándose lentamente, al sistema geotermal y contribuyeron a la formación de la anomalía magnética.

PALABRAS CLAVE: CVM; Cuitzeo; Sistema geotermal; Geofísica; Gradientes direccionales; Campo Volcánico Michoacán-Guanajuato.

ABSTRACT

For the development of a geothermal field, the understanding of fracture distribution, hydrology and tectonic evolution of the site through structural characterization of the natural system is a prerequisite to the drilling of exploratory wells. In order to image the underground shape of

**Corresponding author*
albertomazzoldi@yahoo.com

[1]Instituto de Investigaciones en Ciencias de la Tierra
Ciudad Universitaria, CP 58060
Morelia, Mich., Mexico

[2] EDRA
Via di Fioranello 31, 00134
Roma, Italy

approximately planar, relatively permeable, geologic features (fractured rock-volumes around fault planes) and to detect hot rock volumes, geologic and geophysical surveying is carried out. A strong positive magnetic anomaly, nearly circular in 2D, characterizes the middle of Cuitzéo lake, Michoacán, Mexico, apparently not related with a volcanic structure on the surface. It may instead be associated to the geothermal system in the area which yields at present hot springs at the southern shore of the lake, at boiling temperatures. In this study, we conducted a ground magnetic survey within and around Lake Cuitzeo with the aim of characterizing this anomaly, following one-kilometer-spaced survey-lines and covering an area of approximately 100 km2. To enhance interpretability, we applied computational filters based on directional derivatives (vertical and horizontal) to our reduced-to-pole magnetic-field raw data – illuminating underground faults and other permeable pathways for fluids and delineating contacts between differently magnetized rocks, through maxima and minima on maps. While most filters used were able to define the basic configuration of the system, we found that computational filters working with ratios of derivatives (vertical and horizontal) were able to better account for the depth of a magnetic source. Also, faults were more clearly imaged on maps. We could mainly highlight ~E-W and ~N-S striking fault-systems, respectively belonging to the ~N-S Trans-Mexican Volcanic Belt extensional tectonics and to the ~E-W Basin & Range, both with lateral movements and still active today. We interpret the magnetic source as a magma body (related to the volcanism of Michoacán-Guanajuato Volcanic Field) that remained trapped during its ascent under Cuitzeo lacustrine sedimentation, during the last 500 ka, forming the once stronger geothermal system.

KEY WORDS: TMVB; Cuitzeo; Geothermal system; Geophysics; Directional gradients; Michoacán-Guanajuato Volcanic Field.

INTRODUCTION

Geothermal energy exploits the Earth's natural heat for power generation. It is a low-carbon, base-load alternative energy that, despite its low cost relative to other energy sources, is not yet widely used (Goldstein *et al.*, 2011): financial risk associated with locating and developing the resource – which means understanding the underground shape of permeable features such as faults, for their exploitation – have represented so far, together with environmental impacts, main barriers (Subir and Morrow, 2011; IFC, 2013). Geophysical techniques are often useful for discovering unknown subsurface conditions and can be utilized as preliminary screening before performing direct investigations. Non-invasive potential methods – such as gravity and magnetics – are often appropriate for locating structures (e.g. Glen *et al.*, 2008) and in the general characterization of an underground (geothermal) system, aiming to its exploitation (Pipan *et al.*, 2010; Kipsang, 2015). During the last five decades, a variety of methods based on the use of vertical and horizontal gradients of potential-field anomalies have been developed and implemented for the determination of geologic boundaries, such as contacts and faults – hence also valuable for the exploration of geothermal resources (Nabighian, 1972, 1974; Keating and Pilkington, 1990; Ferreira *et al.*, 2013).

In the trans-tensional sector of the Great Basin, Basin and Range (B&R), western USA, the importance of characterizing known geothermal resources is heightened by the fact that most of the still-undiscovered geothermal systems (~75%) may show no surface hydrothermal springs,

thus defined as blind or hidden (Coolbaugh *et al.*, 2006; Faulds and Hinz, 2015). Faulds *et al.* (2010; 2012) categorized almost 250 geothermal fields in the Great Basin and found that the most favorable tectonic setting for the existence of a system is associated with the presence of a (major) normal fault: geothermal fluids flowing preferentially at fault tips and in fault interaction zones. These zones are characterized by a high density of fractures and dynamically-maintained permeability (Curewitz and Karson, 1997; Rowland and Sibson, 2004; Cashman *et al.*, 2012).

Through the study of aerial data collected along the Surprise Valley, CA (North-West Basin & Range), Glen *et al.* (2013) identified an intra-basin magnetic high, running a significant length of the valley, which they interpreted as a buried, faulted mafic dyke. All the geothermal manifestations in the valley seem to be related to this body as they lie where the high is cut by perpendicular faults (Glen *et al.*, 2013).

In this paper we examine an area within the central Trans-Mexican Volcanic Belt (TMVB, Figure 1), in the northeastern part of the Michoacán-Guanajuato Volcanic Field, a sector interested by, approximately, N-S, E-W, NW-SE and NE-SW structures, repeatedly involved in the formation of small, monogenetic and larger, polygenetic volcanoes (Hasenaka and Carmichael, 1985; Suter *et al.*, 1999; Cebriá *et al.*, 2010). We use magnetic data recorded through detailed surface surveying for characterizing a localized positive magnetic anomaly corresponding to a stretch of the central Cuitzeo Lake (Michoacán, Mexico). Southernly, on the lake shore, hydrothermal manifestations reveal the presence of a geothermal system of medium enthalpy at depth (Arredondo-Fragoso, 1983; Campos-Enríquez *et al.*, 1988).

In the following, we first give a broad review of the regional geology, describing the different tectonics interesting the area. We then apply filters based on combinations of directional derivatives to magnetic data surveyed in the study area, for structural interpretation and with the aim of identifying the heat source and the local structures that allow the rise of the geothermal fluid. We eventually try to give a volcanological explanation for the presence of such heat source at depth.

GEOLOGIC SETTING

The study area is located within the central segment of the TMVB, between 99º and 102º W longitude, Figures 1 and 2. Regionally, the area is interested by the northward extension of the arc, carried by ~E-W striking normal faults with a minor but consistent left-lateral slip component (Suter *et al.*, 1995a; Ego and Ansan, 2002; Garduño-Monroy *et al.*, 2009). From Oligocene times, this territory has been affected by two main trends of subduction-arc related volcanism and the related sin- and post-volcanic extensions, nearly perpendicular to each other. These are the NNW–trending Sierra Madre Occidental volcanic province and the roughly East-West–trending Trans-Mexican Volcanic Belt (TMVB). The two volcanic belts overlap between the Pacific coast and the longitude of Mexico City (Figure 1a) and have at least two characteristic features in common: the broad orientation of the arc and the dominant composition of the rocks (Ferrari *et al.*, 1999).

1 Sierra Madre Occidental volcanic and Basin and Range extensional provinces

The Sierra Madre Occidental (SMO) of western Mexico is a huge Silicic plateau which runs a NNW-trending direction for over 2000 km, from south of the TMVB to the MX/USA boarder (Ferrari *et al.*, 1999; Ferrari *et al.*, 2000). It is the result of Cretaceous-Cenozoic magmatic and tectonic episodes related to the subduction of the Farallon plate beneath the North American Plate (NAP). The rapid increase of the subduction angle during the removal of the plate generated a flux of uprising hotter astenospheric magma, underplating the NAP and intruding within the lower crust (Ferrari *et al.*, 2002), allowing for the extrusion of >300,000 km3 of silicic material (Huppert and Sparks, 1988; Ferrari *et al.*, 2007), apparently erupted from fissure vents corresponding to Basin & Range faults traces (Henry and Aranda-Gomez, 1992; Aguirre-Díaz and Labarthe-Hernández, 2003).

The extensional phases that followed the main volcanic peaks and aged about 30, 23, 10 and 5 Ma (Ferrari *et al.*, 1999) have been sufficiently intense (up to 100%) in the northern part of the SMO (northern Mexico, Figure 1a) to exhume part of the Proterozoic crystalline basement (Dickinson and Lawton, 2001; Ferrari *et al.*, 2007), whereas in the reminder of the arc, and particularly within the southern B&R province, extension has not exceeded 20% (Henry and Aranda-Gomez, 1992; Aranda-Gomez and McDowell, 1998), achieving in the Mesa central, north of TMVB (Fig. 1a), a maximum of about 8% (Nieto-Samaniego *et al.*, 1999).

While an ignimbrite from the upper part of a 300 m thick rhyolitic succession 15 km south of the city of Morelia has been dated by K-Ar at 21±1 Ma (Pasquaré *et al.*, 1991), B&R faults allowing for the extrusion of SMO lavas and aged between 38 and 25 Ma are widespread south of the TMVB (Alba-Aldarve *et al.*, 1996; Morán-Zenteno *et al.*, 1999). Garduño-Monroy and Gutiérrez-Negrín (1992) noted how the regional NNW-SSE B&R Taxco-Queretaro fault, passing some tens of kilometers east of Morelia, represents the eastern limit of SMO volcanism and of the Guerrero Terrain (Campa-Uranga and Coney, 1983).

Seismicity, high heat flow and recent volcanism indicate that the Basin and Range province is actively extending, within its northern and southern parts (Parson, 1995).

2 Trans-Mexican Volcanic Belt and subduction of Fracture Zones

The TMVB is an east-west, Late-Miocene to Quaternary mostly calc-alkaline continental volcanic arc of more than 1000 km longitudinal length and up to 150 km N-S width, originated by the subduction of the Rivera and Cocos plates under the North American plate (Nixon, 1982; Garduño-Monroy *et al.*, 1993; Ferrari *et al.*, 2012), Figure 1b. The mean elevation of the arc is >1500 m with respect to the southern forearc region; summit elevations are between 3000 and 5700 m (Suter, 1991). TMVB presents high mean heat flow (>80 Wm^{-2}; Prol, 1991) and the combination of this with features such as a negative regional Bouguer anomaly (Urrutia-Fucugauchi and Flores-Ruiz, 1996), volcanic activity, sin- and post-volcanic shallow extensional faulting and seismicity, suggests that its central E-W Chapala-Tula fault system may correspond to a young active continental rift (Luhr *et al.*, 1985; Marquez *et al.*, 1999). To the point that Verma *et al.* (2009) coined the terminology 'Mexican Volcanic Rift'.

Along the arc, volcanoes are distributed with a ~15° oblique trend relative to the Middle American Trench (MAT, Figure 1): this suggests that their location is controlled by the slab

geometry (Pardo and Suarez, 1995; Ego and Ansan, 2002; Ferrari *et al.*, 2012). Particularly, the area of Mexico inland of the MAT can be split into several sections with different subduction angles (from W: Jalisco block, JB, 50o; Michoacán block, MB, 30o; Guerrero block, GB, 0o until the latitude of Mexico City and Oaxaca block, 30o. Pardo and Suarez, 1995; Stubailo *et al.*, 2012. Fig. 1b).

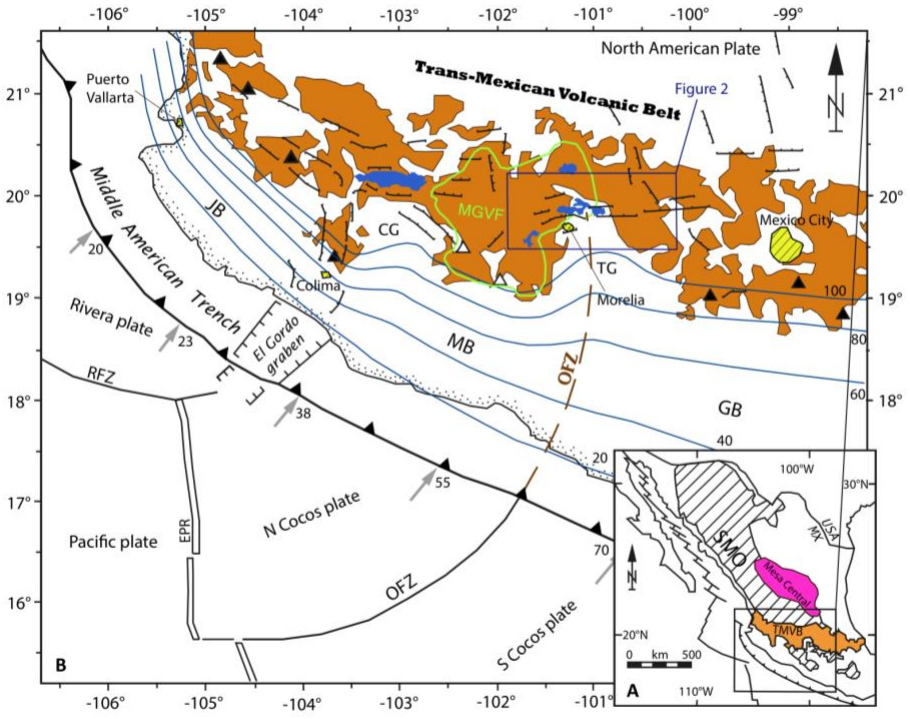

Figure 1 A) The two main volcanic provinces interesting Mexico, Sierra Madre Occidental (SMO) and Trans-Mexican Volcanic Belt (TMVB). For reference, also pictured is the Mesa Central area and the Mexico/USA border. B) TMVB volcanism (brown). With black triangles are located active volcanoes – white triangles represent Paricutin and Jorullo cinder cones at the southern extension of the Michoacán-Guanajuato Volcanic Field (MGVF, green line). Isobaths of the Cocos and Rivera plates (blue lines) follow the subduction of Rivera and Orozco Fracture Zones (RFZ and OFZ). JB=Jalisco Block; MB=Michoacán Block; GB=Guerrero Block; CG=Colima Gap; TG=Tzitzio Gap. Gap. Numbers near arrows along the Middle American Trench indicate subduction speed, in mm/yr.

The Rivera Fracture Zone (RFZ) is generally recognized as the Rivera-Cocos Plates Boundary (RCPB, DeMets *et al.*, 1990; Bandy *et al.*, 1995), it can be dated at 10 Ma as the Rivera plate (Bandy, 1992; Stubailo *et al.*, 2012) and is interested by higher heat fluxes than the surrounding oceanic crust. Gravity, heat-flow and sea-morphology analyses suggest that the subducted part of the RCPB lies directly beneath and is oriented parallel to the Southern Colima graben (Bandy, 1992). Bandy *et al.* (1995) showed that the RCPB lies east of the Central and Northern Colima graben and is related to the Colima Gap (CG, Figure 1b), coinciding in plan with the area where the Wadati-Benioff zone undergoes a sharp decrease in dip, eastward. These authors suggested the presence of a NE-SW oriented tear-fault between the subducting plates, explaining the low density zone beneath the granitic highlands (CG) by thermal convective movements in the upper mantle, providing a conceptual model consistent with roughly E-W extension within the subducting lithosphere (Nixon, 1982; Bandy, 1992; Ferrari *et al.*, 1994).

Easterly of the RFZ, Stubailo *et al.* (2012) confirmed previous results (e.g., Pardo and Suarez, 1995; Blatter *et al.*, 2007) that the angle of subduction varies substantially at the longitude of the Tzitzio Gap (TG, figure 1b), consistent with the location of the Orozco Fracture Zone (OFZ, Fig. 1), which separates older (17.6 Ma), cooler and denser oceanic crust at the NW side from younger crust (12.3 Ma) at the SE (Manea *et al.*, 2005). Slab rollback (retreat) below the MB occurs at about 5 cm yr^{-1} (Singh and Pardo, 1993; Bandy *et al.*, 2000; Suter *et al.*, 2001): this process should displace mantle asthenosphere, and, in the presence of a slab tear, the mantle material would flow through it. Tear faults occur where the plate is weakened by the presence of the fracture zone.

During subduction, fracture zones are buoyant enough to usually lower the angle of descent of the subducting plate: the arc volcanism is consequently displaced landward, creating indentations in the front of the volcanic arc (McCann and Habermann, 1989). Through vulcanological studies, Blatter and Hammersley (2010) concluded that the OFZ is being subducted under the TG and that the buoyancy of the fracture zone would cause this section of the Cocos slab to subduct at a lower angle than the Cocos slab on either side of the OFZ. This causes the subducting material to reach the melting depth of about 100 km at higher distance from the trench, in correspondence with the OFZ (and TG), spatially 'delaying' volcanism at the surface towards the north. Dougherty *et al.* (2012) proposed that the Cocos slab is currently fragmenting into a N Cocos and a S Cocos plates along the projection of the OFZ, in agreement with other authors (Bandy, 1992; Bandy *et al.*, 2000). They identified this tearing event as a younger (~0.9 Ma) analogy of the 10 Ma old Rivera-Cocos plate boundary.

3 Structural geology, regional seismicity and state of stress of central TMVB

The central part of the TMVB (99°-102°W) is characterized by major E-W intra-arc basins: from W to E, the Chapala, Cuitzeo, Acambay and Mezquital grabens, 8-10 Ma old (Garduño-Monroy *et al.*, 1993; Rosas-Elguera *et al.*, 1997), whose E-W to ENE-WSW bordering normal faults have mean Quaternary slip rate of <0.1 mm yr^{-1}, characterizing the area with a ~N-S oriented extension of <5% (Suter *et al.*, 1995a; Ferrari and Rosas-Elguera, 2000). Recent studies have proposed, for some of these structures, an age of 18 Ma (Mendoza-Ponce *et al.*, 2018). Figure 2 shows the Acambay and Cuitzeo extensional areas. The Acambay graben is a ~30 km long E-W structure with delimiting faults dipping 50°-70°, with a mean slip rate of 0.17 mm yr^{-1} during Holocene times (Langridge *et al.*, 2000). Cuitzeo graben (and half-graben) can be traced for over 45 km and its master faults dip between 45° and 75° (Ferrari *et al.*, 1991; Garduño-Monroy *et al.*, 2009. See Figure 3), having slip rates between 0.09 and 0.18 mm yr^{-1}, which is approximately three times higher than in the Morelia area, 20 km south (Suter *et al.*, 2001). E-W fault planes' striations indicate an extensional (N-S) dip-slip with a left-lateral strike-slip component (Pasquaré *et al.*, 1988; Garcia-Palomo *et al.*, 2000), which was explained by Ego and Ansen (2002) with slip-partitioning at the trench.

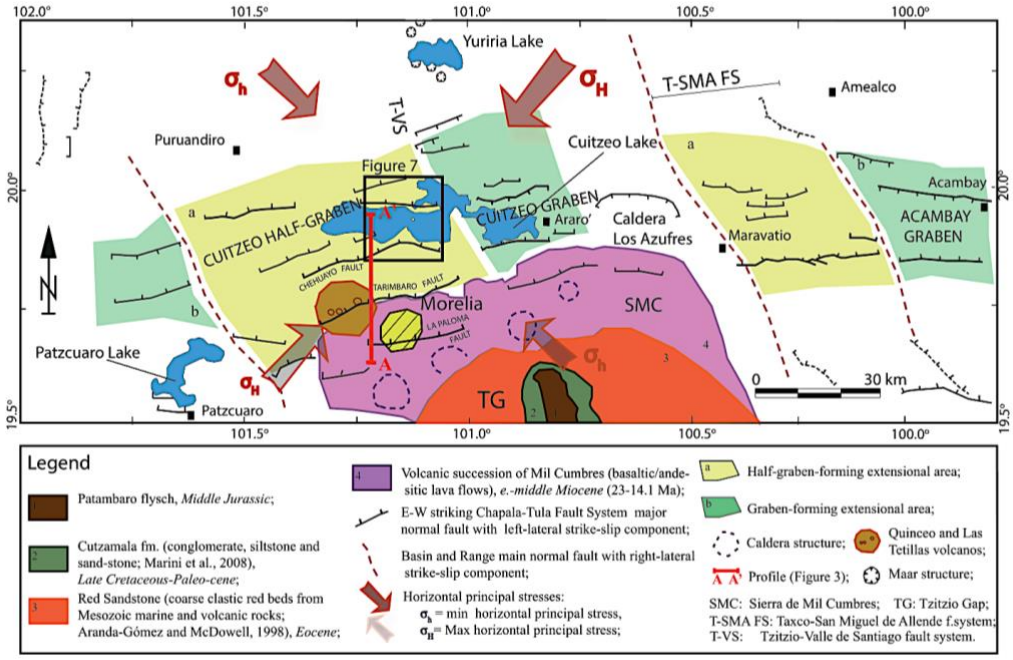

Figure 2. Cuitzeo graben and half-graben, representing the proto-continental rift structure of the Chapa-Tula fault system, cut by regional NNW-SSE normal structures with right lateral sense of shear, belonging to the southern Basin & Range tectonics. Also represented are the Tzitzio Gap (TG) and Sierra de Mil Cumbres (SMC) in the south and some Maars structures in the north, around Yuriria lake. Centrally, the Cuitzeo basin and the area of study (black box). Image modified after Garduño-Monroy *et al.*, 2009.

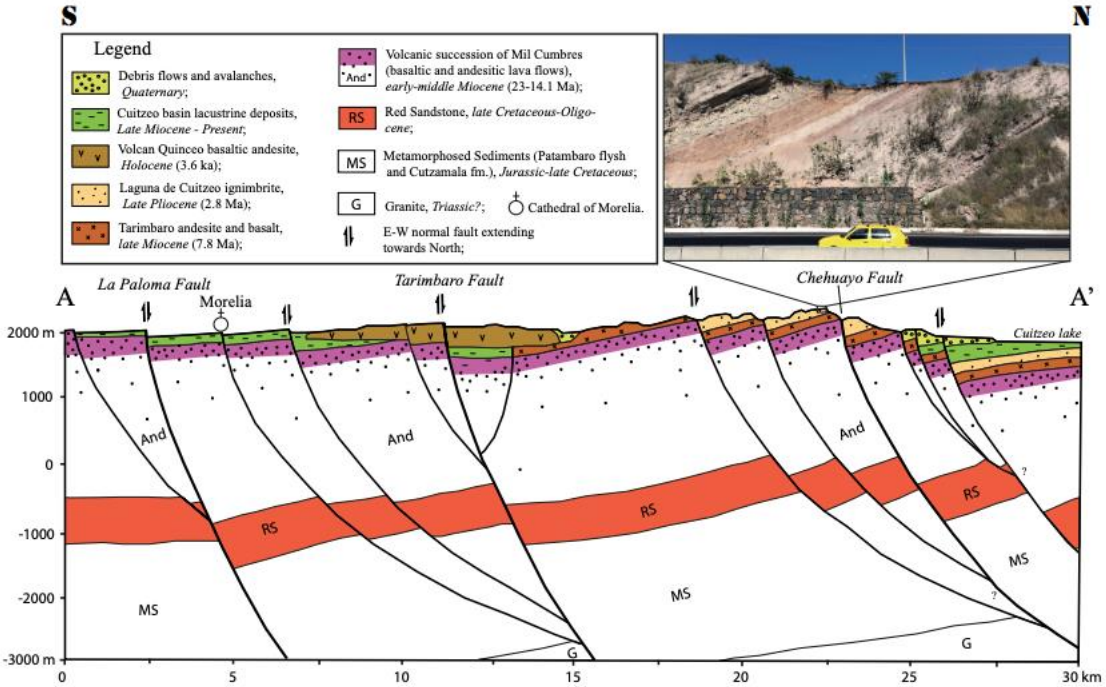

Figure 3. Geologic profile AA' from Figure 2. Evident are the E-W listric normal faults causing minor extension (<5%, see text). The stratigraphy under Cuitzeo lake sedimentation is mainly composed of TMVB-basamental andesite of basic and intermediate nature.

Central TMVB is seismically active (Suter *et al.*, 1996; Garduño-Monroy *et al.*, 2009) and during the last century, eight shallow events with magnitude 4.1<M<6.9 occurred along E-W faults; among these, the Acambay, 1912 (M=6.7) and the Maravatio, 1979 (M=5.3) earthquakes (Suter *et al.*, 2001).

Southern B&R NNW-SSE structures present a normal-right-lateral sense of motion (Garduño-Monroy and Gutierrez-Negrin, 1992; Garcia-Palomo *et al.*, 2000). Historical seismic events of Mw>3 comprehend the Pinal de Amoles (1887) and the Sanfandila (1998) events (Suter *et al.*, 1996; Zuñiga *et al.*, 2003) and Peñamiller sequence (2010-2011; Clemente-Chavez *et al.*, 2013). Although we do not have data on mean slip rates, Alaniz-Alvarez *et al.* (1998) determined how, on average, north-south B&R faults only have about one-third of the horizontal displacement rate of the east-west TMVB faults. The contemporaneous activity of TMVB and B&R faults in the area was explained with a recurrent permutation of σ_1 and σ_2 (see figure 2, where $\sigma_1=\sigma_V$) which would allow for the activation of NNW-striking B&R structure as right-lateral during the deposition of the Cuitzeo (and Acambay) basin sedimentation (Suter *et al.*, 1995b; Ego and Ansan, 2002).

3.1 The Michoacán-Guanajuato Volcanic Field

A monogenetic volcanic field, covering an area of some 40,000 km^2 is located at the west-central sector of TMVB, extending over northern Michoacán and southern Guanajuato and interesting the study area (Figures 1 and 4). A unique part of TMVB for its lack of young large composite volcanoes, dominant in the rest of the arc, the Michoacán-Guanajuato Volcanic Field (MGVF) has been active from Pliocene to present (Hasenaka and Carmichael, 1985; Ferrari *et al.*, 2007). It contains more than 1000 small volcanic centers, as shown in Figure 4, and its main eruptive products are calc-alkaline olivine basalt and basaltic andesites (Hasenaka and Carmichael, 1987): rocks crystallized from these magmas can hold relatively high abundances of ferromagnetic minerals. The majority of the small-sized volcanoes are cinder cones (~900) but the field also comprehends lava domes, maars, tuff rings and thick lava flows not associated with cones (Williams, 1950; Hasenaka, 1994), coexisting in time and space with over 300 medium-sized shield volcanoes distributed throughout the volcanic field and whose origin may not be univocal (monogenetic or polygenetic. Hasenaka *et al.*, 1994; Verma and Hasenaka, 2004). While small volcanic centres in MGVF are spread all over the extension of the field, authors have identified alignments of cones following geological structures (Cebriá *et al.*, 2010; Gomez-Vasconcelos *et al.*, 2015), implying that, although volcanism may be a consequence of contemporaneous extensional regimes, the distribution of monogenetic vents is actually controlled by reactivation of older fractures, producing space for magma ascent at near surface levels (Hasenaka and Carmichael, 1985).

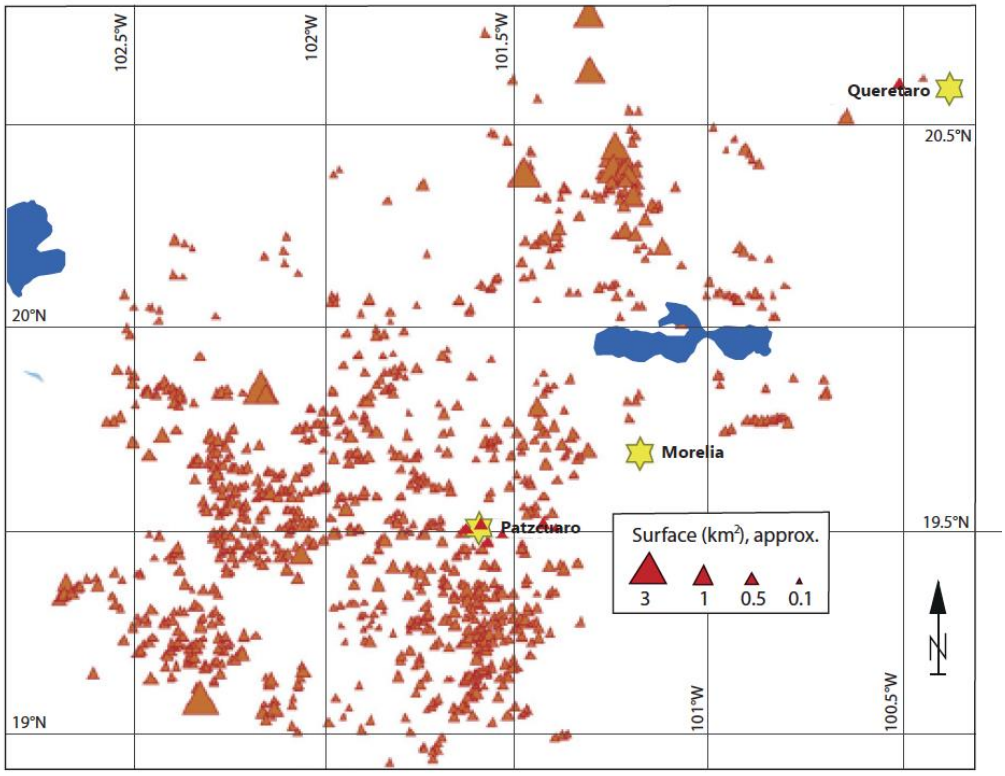

Figure 4. Extension of the Michoacán-Guanajuato Volcanic Field, with an approximate description of cone dimensions (data from Pérez-Lòpez *et al.*, 2011).

Through geochemical and isotopic studies of rock samples from the whole extension of the MGVF, Verma and Hasenaka (2004) concluded that no slab input is present in the basic magmas of the field and that different degree of partial melting of a heterogeneous mantle source could explain the origin of most magmas in the field, allowing for some crustal assimilation for the most evolved – supported by the presence of frequent granitic xenoliths (Verma and Hosenaka, 2004, and references therein).

4 Regional geophysics and the study area

Figure 5 presents the relative Bouguer anomaly with respect to the WGS84 across the area within and around the Cuitzeo Basin. This map is based on data of Petroleum of Mexico (Pemex) from 1980 (Arredondo-Fragoso, 1983). The lowest values of the gravity field within the lake are linked with relatively light lacustrine sediments (density, $\varrho \cong 1.7$ Kg m^{-3}) and may then correspond in plan to the depocenter of the lake (where sedimentation has been highest during the past 8-10 Ma), with an estimated thickness of about 1.5 km. Positive anomalies, S and NE of the lake, are respectively linked with the Sierra de Mil Cumbres (SMC) and the Sierra the San Andres (SSA) ranges, built through eruptions of andesitic material ($\varrho \cong 2.7$ kg m^{-3}).

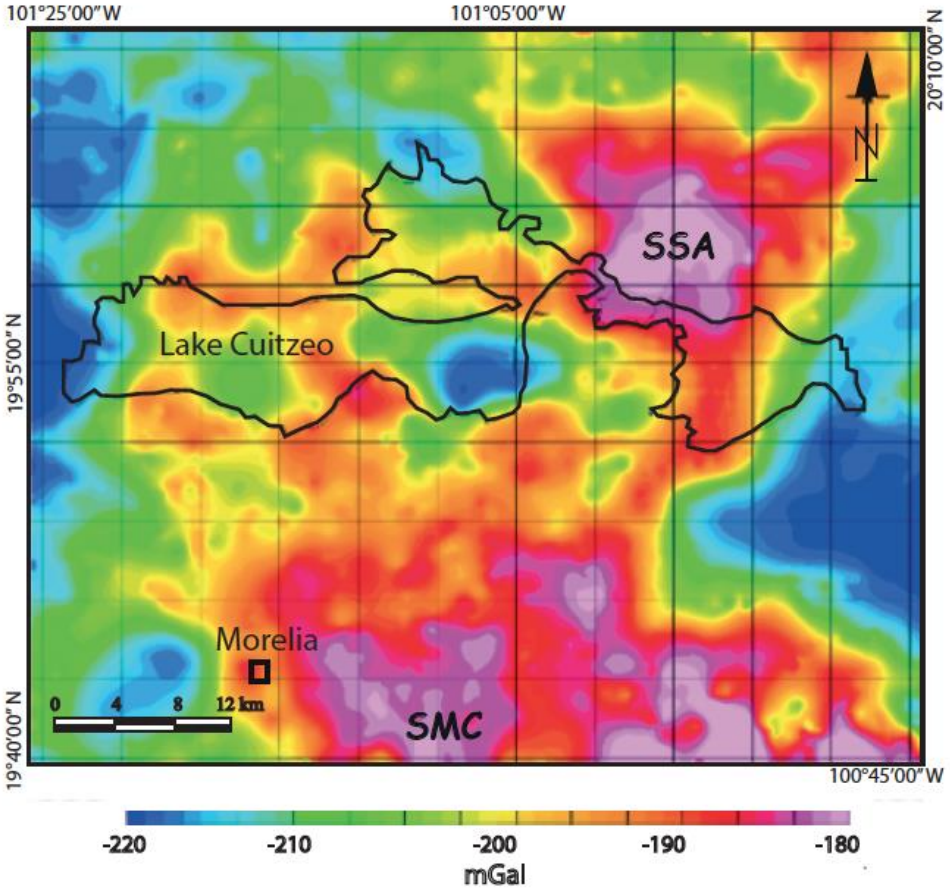

Figure 5. Map of anomalous values of gravitational acceleration in the area of the Cuitzeo lake. Peaks are related with the Sierra de San Andrés (SSA), northeast of the lake, and Sierra de Mil Cumbres (SMC), south. Regional lows border the area longitudinally while, in the middle of the lake, low values are located above the depocentre of the basin.

Figure 6 shows the reduction to the pole of the regional magnetic field around the study area, from aeromagnetic data of the Mexican Geological Survey (Servicio Geológico Mexicano, 1988). The magnitude of an anomaly in the magnetic field recorded at the surface, with respect to the International Geomagnetic Reference Field (IGRF; Thebault *et al.*, 2015) mean value, is dependent on the concentration of ferromagnetic minerals in the rocks of the upper crust at the site (Jackson and Bowies, 2014). Strong positive anomalies may then be related with large volumes of rock of basic composition (andesitic/basaltic solidified magmatic bodies), below Curie temperature for magnetite (around 575$_{o}$C) and crystallized after the Matuyama-Brunhes reversal, about 780 ka (or during any other period of normal polarity), outcropping at the surface or trapped within the shallow crust. Cuitzeo basin is bordered by different magnetic highs linked with volcanic edifices at the surface (Figure 6), particularly the SSA, NE of the lake.

A relatively strong positive magnetic anomaly lies in the middle of the actual lake, some hundreds of meters NW of the gravity low, in plan. The origin of this anomaly may be found in a volcanic structure older than the lake and consequently covered by the lake sediments, or it may be correlated to an ascending magma body, blocked by the plastic lacustrine sediments.

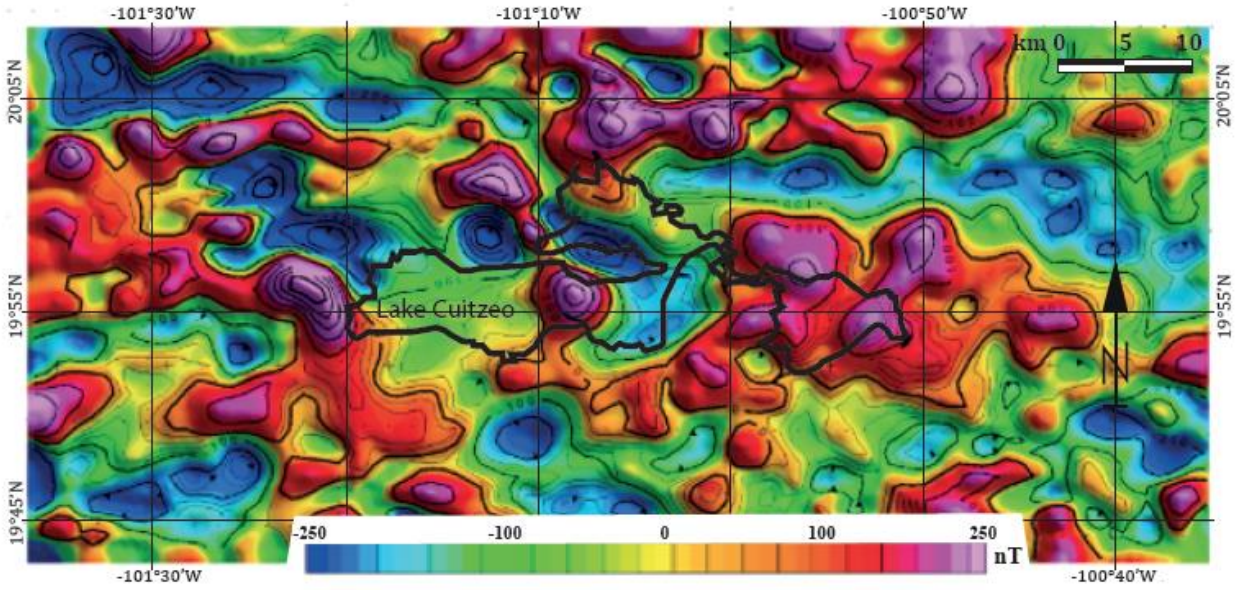

Figure 6. Regional magnetic anomaly (vs IGRF values) map. Positive anomalies around the lake are related with volcanic edifices built with basic and ultrabasic magmas. In the middle of the lake, slightly NW with respect to the gravimetric low, a positive anomaly is studied in this work.

In Figure 7a principal lithologies and main structures are presented: massive andesitic and ignimbritic highly fractured banks outcrops in the area (Fig. 7b and c). Our structural survey showed a statistical prevalence of ~E-W fault planes on outcrop, with dips <75º. Nearly vertical ~N-S striking fault planes (showing horizontal striae and with fractures completely sealed by hydrothermal calcite) outcrop in an area south of San Juan Tararameo (SJT, Figure 7d), denoting the existence of a paleo-geothermal system. In the image, inferred continuations of some of these structures below the lake are shown with dotted lines and an andesitic island can be seen in the center of the image. Shown are also the areas interested by geothermal manifestations, with more than 100 springs between San Agustin del Mais (SAM) and SJT, laying near faults intersection (Sibson, 1981; Rawland and Sibson, 2004) and marking the areas with long-lived siliceous sinter terraced-deposits, associated with high temperature hydrothermal reservoirs (Fournier and Rowe, 1966).

Water temperatures of the springs reach 93ºC (our work), water-boiling T at the location (1820 m a.s.l.). A geochemical study of different geothermal springs around lake Cuitzeo (Segovia *et al.*, 2005) found at SAM and SJT steam heated waters in partial equilibrium, observing a mixing trend among the samples – indicating reservoir temperatures between 150 and 220ºC. Their Radon analysis results indicated a highly efficient fluid flow transport in the zones where higher temperatures were estimated. Lastly, the 8 NE-SW traces over which magnetic measurements were taken, as described in the following, are also depicted in Figure 7.

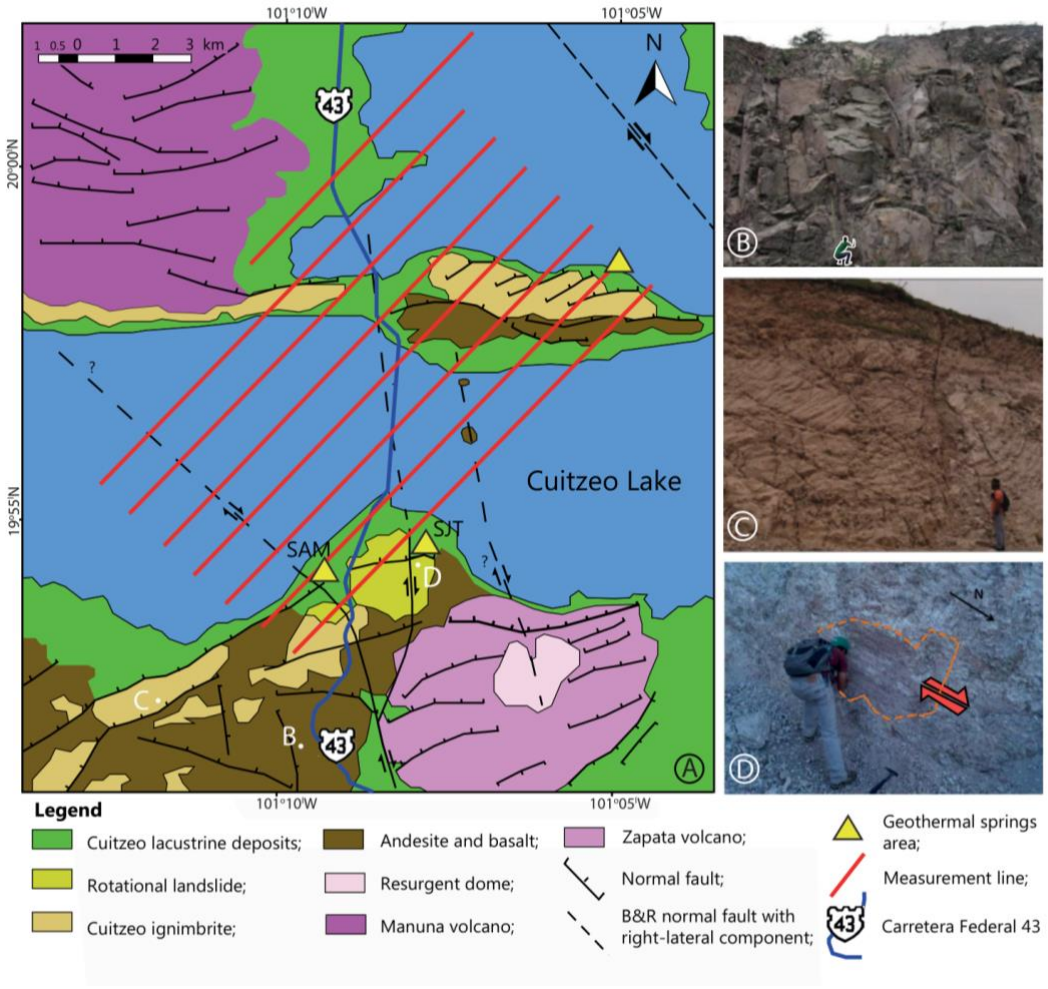

Figure 7 a) The area of study. Represented in the picture is the geological map of this territory with traces of known and supposed fault lines. Also located are the neighborhoods endowed with geothermal springs and the eight lines followed by our magnetic survey. b) Andesite block outcropping. c) Ignimbritic blocks. d) Right-lateral strike-slip fault plane within the andesitic basement, filled with deposition of geothermal calcite.

MAGNETIC SURVEY: DATA ACQUISITION, PROCESSING AND INTERPRETATION

Survey lines, spaced 1 km, were 15 km long but the northern one (reduced to 8 km, Fig. 7a) and were covered on foot and by rowboat (made of plastic and wood for not affecting measurements), from May 2015 to July 2016. Measurements of magnetic field where taken at stations spaced 100 m on each line, using a Geometrix G-857 proton-precision magnetometer, connected with a Garmin Oregon 450 GPS that guaranteed each measure to be taken within 2 meters from the station location, on each line. Different stations could not be covered due to the presence of anthropic barriers, corrupting measures in their proximities (e.g., buildings and other constructions, power lines), leaving a total of 975 point-values for analysis, over an area of some 110 km2. Instrumentation also comprehended an independent base-station for calculating daily variations of the magnetic field due to solar wind interferences during working hours, recording values at a fixed point. Due to theft of the base-station, we used the values of the

Magnetic Observatory of Teoloyúcan to make diurnal corrections to our data, during the last part of the survey.

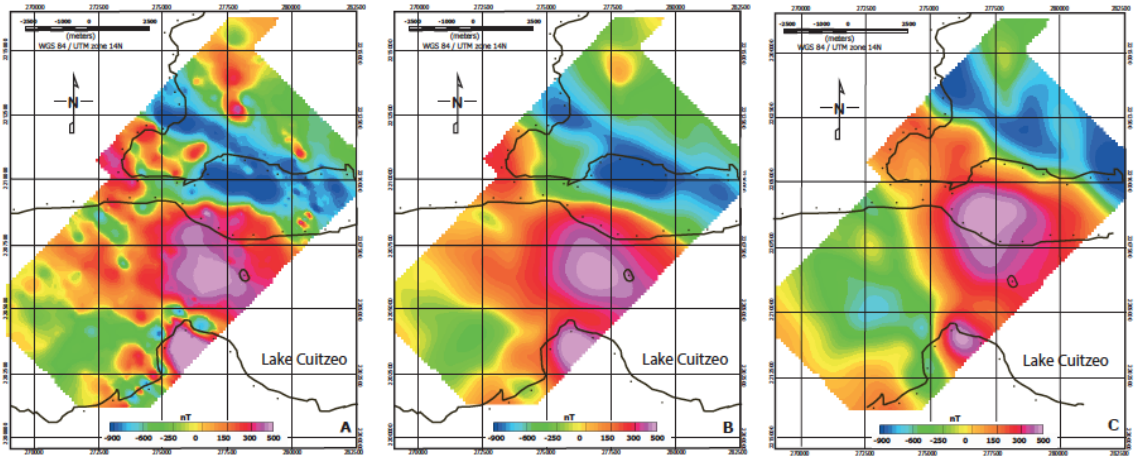

Figure 8 a) Map displaying raw values of the magnetic anomaly (relative to the IGRF) recorded along the measurement lines. Superimposed is Cuitzeo lake-shore contour. b) Upward Continuation at 500 m depth (see text for explanation). c) Reduced-to-Pole values after Upward Continuation; derivative-based computational filters have been applied on this value-grid.

We worked on the magnetic raw database (after correcting for daily variations) using the software Encom Discover PA 2010 (®RockWare). We applied to the mapped dataset computational filters based on operations with directional derivatives of the data, as described in the following. Figure 8a maps the anomaly values of the Total Magnetic Field, relative to the IGRF, displaying a positive anomaly in the middle of the surveyed area.

Surface data suffer from high-frequency noise due to shallow sources and probably also due to higher-than-optimum stations separation, for some stations. One of the tasks of data processing is to simplify the complex information provided in the original data: we have applied to our data an Upward Continuation (UC) filter, a low(wave-frequency)-pass filter which allows to avoid considering the contribution to the total magnetic field recorded at the surface given by rock layers above a certain depth (e.g. Gianiyu *et al.*, 2013, Ferreira *et al.*, 2013). Specifically, the filter was applied to the data-grid for the depth of 500 m in order to discard the contribution of high-frequency shallower potential sources to the recorded magnetic field values, as shown in Figure 8b. The filter Reduction-to-Pole (RP) is utilized to image measured values as if the measurements were taken at the magnetic pole: it reduces bipolar anomalies to monopolar ones, considering magnetic Inclination and Declination at the site (respectively 47° and 7° for the study area), basically placing anomalous values of the magnetic field on the vertical of the geological bodies causing them (Baranov, 1957). The application of the RP filter to UC data is shown in Figure 8c: these data have been used as the basis for the application of the mathematical filters described below.

Local magnetic field of the study area, upward continued and reduced-to-pole, presents a principal positive anomaly (reaching values higher than 400 nT with respect to IGRF) sited near the center of the area (Figure 8c) which is potentially due to the underground geologic body we aim to characterize. Also present is a smaller peak, south of the principal one, which might be related with the volcanic stratigraphy of the shore.

1 DATA FILTERING: OPERATIONS WITH DIRECTIONAL GRADIENTS

In the last decades, a variety of methods based on vertical and horizontal derivatives of surveyed potential field data have been developed as efficient tool for the determination of geometric parameters of causative bodies (such as location of boundaries and depth-to-top) and structures (i.e. major faults. Nabighian, 1972; Roest *et al.*, 1992; Miller and Singh, 1994; Ravat *et al.*, 2002). The first vertical derivative (VDr) of the magnetic field is the rate of change of its intensity (M in Table 1) in the vertical direction. Its computation removes long wavelength features of the magnetic field and, while it amplifies signals from shallower sources, it significantly improves the resolution of closely spaced anomalies (Hood, 1965). VDr (Equation 1 in Table 1), on a map, has its zero values over the vertical edges of thick source bodies and positive and negative values over positive and negative anomalies (Cooper and Cowan, 2004). In Figure 9a the first order VDr of the UC and RP data is shown, together with the representation of a likely anomaly' source edge, drawn approximately following the zero contour. In the image, the magnetic response from the southern anomaly seems slightly heightened.

Table 1. Equations describing computational filters used on magnetic data. See text for explanation.

Equation #	Formula	Measure
1	$VDr = \frac{\partial M}{\partial z}$	$\frac{\eta T}{m}$
2	$2VDr = \frac{\partial^2 M}{\partial z^2}$	$\frac{\eta T}{m^2}$
3	$(VDr)THDr = \sqrt{\left(\frac{\partial VDr}{\partial x}\right)^2 + \left(\frac{\partial VDr}{\partial y}\right)^2}$	$\frac{\eta T}{m^2}$
4	$AS = \sqrt{\left(\frac{\partial M}{\partial x}\right)^2 + \left(\frac{\partial M}{\partial y}\right)^2 + \left(\frac{\partial M}{\partial z}\right)^2}$	$\frac{\eta T}{m}$
5	$(VDr)AS = \sqrt{\left(\frac{\partial VDr}{\partial x}\right)^2 + \left(\frac{\partial VDr}{\partial y}\right)^2 + \left(\frac{\partial VDr}{\partial z}\right)^2}$	$\frac{\eta T}{m^2}$
6	$TA = tan^{-1}\left(\frac{VDr}{THDr}\right)$	rad
7	$(TH)TA = tan^{-1}\left(\frac{\frac{\partial THDr}{\partial z}}{\sqrt{\left(\frac{\partial THDr}{\partial x}\right)^2 + \left(\frac{\partial THDr}{\partial y}\right)^2}}\right)$	rad

The second vertical derivative (2VDr, Equation 2 in Table 1) is used for improving resolution of anomalies and to delineate geological discontinuities in the subsurface. Lineaments in a 2VDr map would lie at value 2VDr = 0, following abrupt change in magnetization due to geologic structures (Rebolledo-Vieyra *et al.*, 2010; Lopez-Loera *et al.*, 2010). In Figure 9b this filter is applied to our data, showing some imaged potential fault-lines following zero contours on the map, where horizontal gradients are highest. Being a second order filter, 2VDr enhances near surface effects at the expenses of deeper anomalies, it amplifies noise and may produce artificial second derivative anomalies (Wahyudi *et al.*, 2017).

Total Horizontal Derivative (THDr) is considered as the simplest approach to estimate contact locations and has been used as edge detector (Cordell & Grauch, 1985, Cooper & Cowan, 2008). It displays maxima above nearly vertical borders of source bodies (or faults with decent offset) and relative minima at the center and outside of sources. Figure 9c shows the application of this filter to the VDr grid (Equation 3), as in Fedi and Florio (2001), where they used the filter

for defining boundaries of a calderic collapse in southern Italy. Superimposed to the map are some interpreted structures.

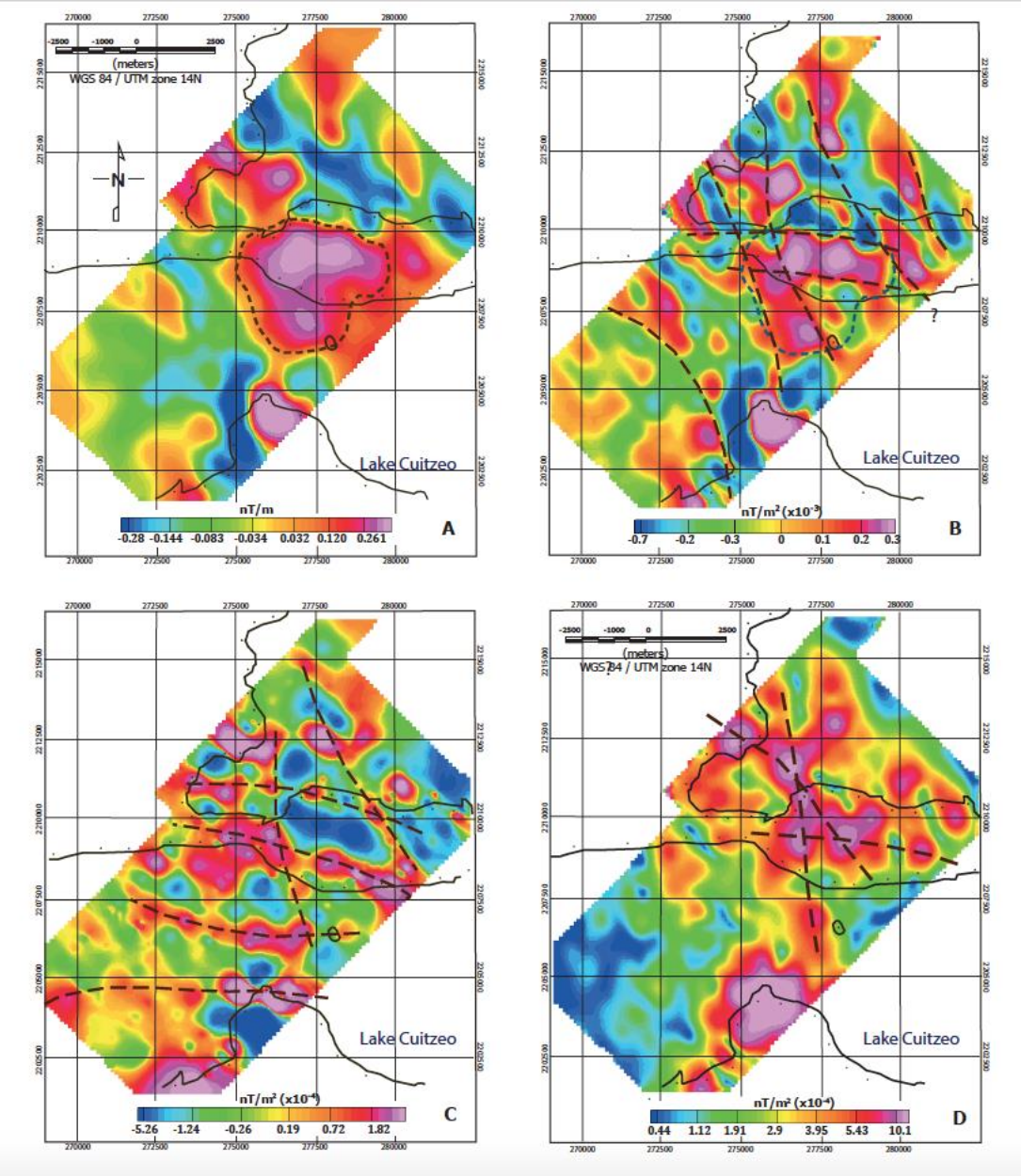

Figure 9. a) First vertical derivative (VDr, equation 1 in Table 1) of the data with contour of the potential magnetic source, interpreted. b) Second vertical derivative (2VDr, eq. 2) applied to our data. Depicted are some potential fault lines, interpreted. c) Total Horizontal derivative (THDr) applied to VDr grid (eq. 3). d) Analytic Signal (AS) applied to VDr grid (eq. 5).

1.1 Analytic Signal

Mathematics, an Analytic Signal (AS) is a complex-valued function that has no negative frequency components. Developed by Nabighian (1972, 1974) and also known as total gradient, the AS amplitude is defined as the square root of the sum of the squared directional derivatives,

as described by eq. 4. AS presents maxima above near vertical magnetic contrasts, identifying faults or geologic bodies of different susceptibility or induced magnetization.

Potential field data correspond to the superposition of all causative sources and nearby source interference yields mislocations (Grauch and Cordell, 1987). Authors have used the filter AS on grids of vertical derivatives of n order (for n = 1, 2) for sharpening nearby boarders (Nabighian, 1972, Roest *et al.*, 1992). Figure 9d displays the AS filter applied to the VDr grid (eq. 5). The signal due to the southern positive anomaly appears strongly enhanced and, while this filter distinguishes between the two anomalies, it only marginally helps in structures identification. From the image we could recognize a N-S and a E-W striking structures crossing near the centre of the picture and a NW-SE structure which we could not recognize through the application of other filters but that may also belong to B&R deformation. Application of AS to higher order vertical derivatives of our data amplifies high-frequency noise to intolerable levels, further attenuating deep source signal.

Since the strength of a magnetic field decays proportionally to source–receptor distance cubed, a handicap of these simple derivative-based filters is that they tend to magnify shallow sources at the expenses of deeper ones, whose gradients measured at surface are weaker. Particularly for our data, the southern anomaly recognized on the RP map (fig. 8c) seems enlarged by vertical derivations (fig. 9a, b and d).

2 TILT ANGLE

The Tilt Angle (TA), introduced by Miller and Singh (1994) for profiled data and improved by Verduzco *et al.* (2004) for 3D cases, overcomes the problem of amplifying shallow sources, which characterizes simple derivative-based filters. This is accomplished by dealing with the ratio of the vertical derivative to the horizontal one, as in Eq. 6. Both VDr and THDr will be smaller for deep sources than for shallower ones, so that their ratio will still be large over the source, pass through zero over or near the edges (where VDr is zero and THDr presents maxima), and will be negative outside of the magnetic body (where VDr < 0), in 2D. Due to the nature of the arctan trigonometric function, all amplitudes are restricted to values between $\pi/2$ and $-\pi/2$ (+90° and -90°) regardless of the amplitudes of VDr and THDr (Miller and Singh, 1994). These facts make this filter function like an automatic gain control (AGC) sieve, tending to equalize the amplitude of the signal for shallow and deeper sources (Verduzco *et al.*, 2004; Salem *et al.*, 2007). The application of the TA to our data is shown in Figure 10. This filter gives the two sources (northern and southern, in the image) balanced leverages: the dimensions of the southern anomaly appear downsized and can be linked with a shallow source (shore' volcanic stratigraphy?).

Salem *et al.* (2007) developed the 'Tilt-depth method' for estimating the depth of a magnetic source from 2D TA maps. They demonstrated how, under certain assumptions such as when contacts (between differently magnetized lithologies) are nearly vertical and the magnetic field is vertical (or RP), contours of TA on a map can help identifying both the edges of magnetic structures (TA = 0) and their depth, as half the physical distance between $\pm\pi/2$ contours. They applied the method on aeromagnetic data over the Karoo sedimentary rift structures of southeast Tanzania (Salem *et al.*, 2007). Applied to our data (Figure 10), the methodology estimates a depth for the roof of the magnetic body (which we argue to equal the depth of the bed of Cuitzeo'

lacustrine sedimentation, at the site) between about 700 and 900 m (depth = AB/2, on the TA map).

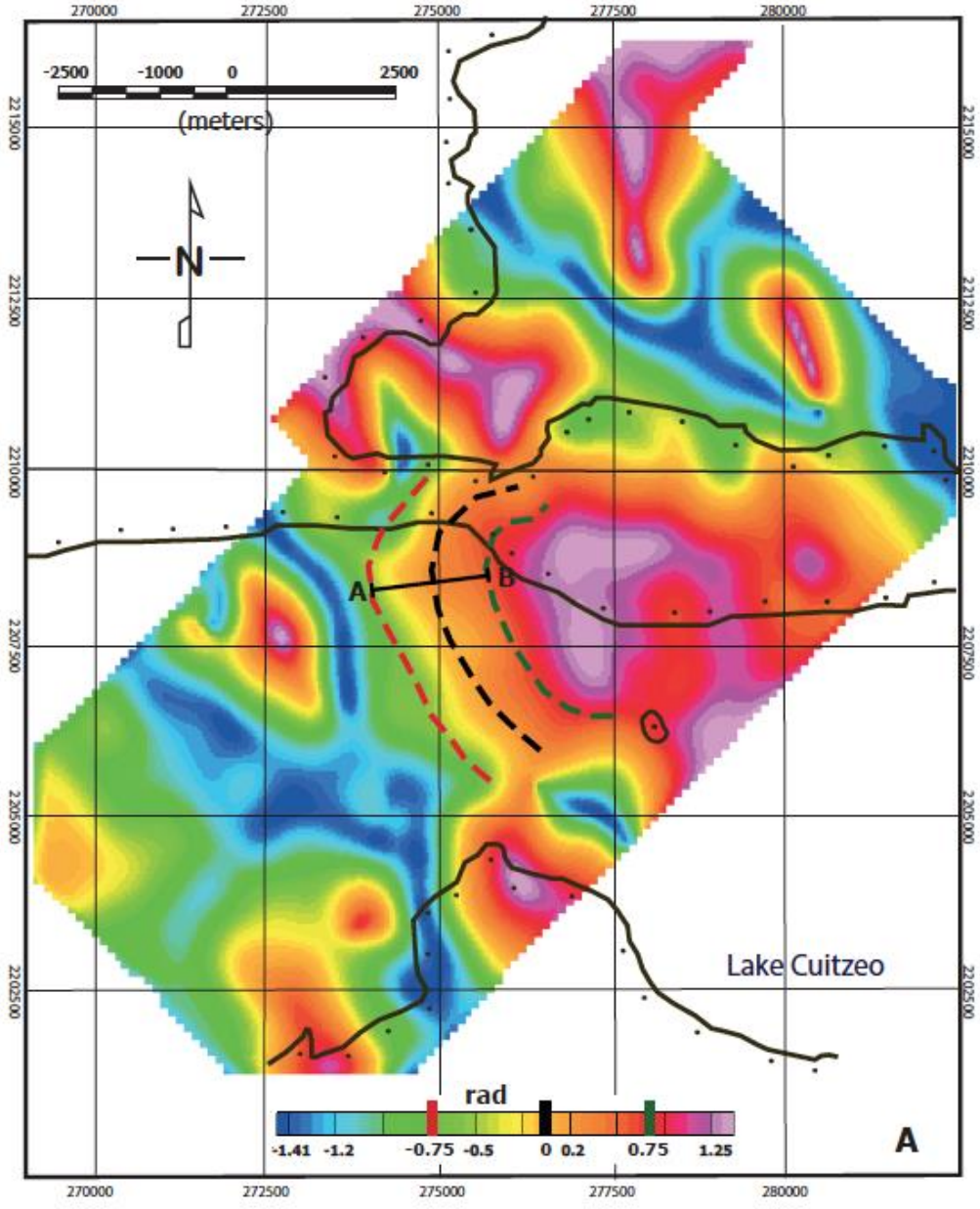

Figure 10. Tilt-Angle (TA, eq. 6) applied to our data. Coloured dotted lines are drawn following the contours TA=-0.75, 0.75 and 0, for the application of the *Tilt-depth* method, described in the text.

2.1 TILT ANGLE OF THE HORIZONTAL GRADIENT

Ferreira *et al.* (2013) presented an edge detection method that is based on the enhancement of the THDr of magnetic anomalies using the TA. Referred to as Tilt angle of the (total) horizontal gradient, (TH)TA was applied by the authors to 3D synthetic models, displaying balanced maxima over the

edges of magnetic prisms located at different depths with outstanding precision, particularly when compared to other edge detection methods. Also, the filter was tested for the detection of edges of superimposed sources (Ferreira *et al.*, 2013), obtaining promising results. The authors applied the filter to aeromagnetic data of an area in the central portion of the Ribeira belt (state of Rio de Janeiro, southeastern Brazil), a Neoproterozoic range consisting of four tectonostratigraphic terranes. Through its maxima, the filter helped in defining major regional faults and shear zones and in characterizing dykes and other intrusions (Ferreira *et al.*, 2011).

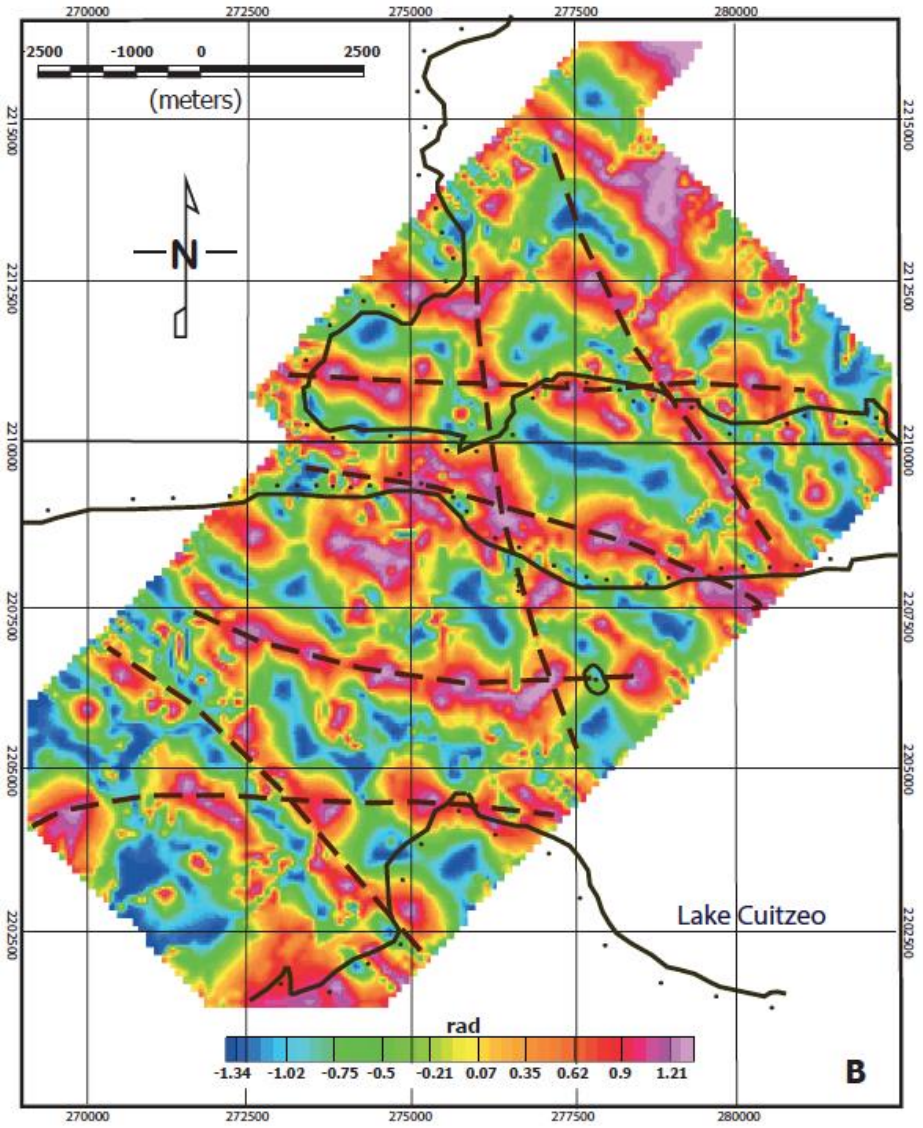

Figure 11. TA applied to the THDr grid, (TH)TA, eq. 7. Superimposed are the traces of some potential fault lines, interpreted.

We applied (TH)TA to our data (eq., 7. Figure 11) and it revealed very useful in locating potential faults, giving support to our structural interpretation. Main TMVB (E-W) and B&R (N-S) faults in our study area, identified by this method through positive sharp peaks, affect the volcanic bedrock (pre-TMVB) and the >8 Ma old lacustrine sedimentation, thicker than 700 m above the magnetic source in study. There are recurrent E-W structures affecting the study area,

one of which interests the Cuitzeo peninsula (Figures 7, 9a, b, c, 11) that, being located on top of the magnetic anomaly in maps, could be directly related to the once hotter magma body, now causing the magnetic anomaly. Particularly, the southern half of the peninsula is made up of lava flows of basic composition (andesite) and is separated from the northern half, constructed with ignimbritic products, by an E-W structure lying approximately in the middle (figure 7a): the two lithologies might have been erupted from the fissure itself, potentially during the same event. On the other hand, we believe that the volcanic island in the middle of the lake may be linked with a N-S structure, as explained in the conceptual model of the system, in the following.

Discussion and Conclusions

The application of filters based on combinations of directional derivatives to magnetic data surveyed over the middle section of Lake Cuitzeo helped in the identification of structures potentially affecting the underground, below and within the cap-rock layer consisting of the basin sedimentation. While the application of the vertical derivatives and tilt angle filters to the data may indicate the presence of a cylindrically shaped magnetic body at a depth shallower than 1 km (Figures 9a and 10), the interpretation of results is based on restricting assumptions (e.g. verticality of lateral borders) which would indeed characterize the magnetic body based on its inherent geometry, related to its nature and origin. The Authors of this work have been criticized on a previous publication (Mazzoldi *et al.*, 2016) in that the magnetic anomaly in the study area may be due to a volcanic structure older than the Cuitzeo lake (8-10 Ma) and submerged by the lake sediments afterward, thus not related with the geothermal system. Transect in Figure 3 shows the stratigraphy below the sediments of lake Cuitzeo, displaying massive amounts of andesitic material constituting the TMVB basement. Authors agree that a TMVB 'basement volcanism', with the same general geometry of the present arc and developed during a time-span comprehending the last activities of SMO and the beginning of proper TMVB volcanism, should be considered as an independent volcanic province (Gutiérrez-Negrín, 1988; Ferrari *et al.*, 1999). With an approximate age between 15 and 7 Ma, its volcanic products would still belong to a calc-alkaline series, but more acidic than TMVB magmas (Venegas *et al.*, 1985; Garduño-Monroy and Gutiérrez-Negrín, 1992), somehow representing a middle member between SMO and TMVB – which contrast with the thesis of the magnetic high being due to a volcanic edifice of ultrabasic composition (needed to justify the anomaly under the lake).

The highly basic and ultrabasic magmas of the MGVF, solidified underground below the lake sediments and forming the studied magnetic anomaly, allowed to shed some light on the structural condition of the geothermal reservoir at Cuitzeo, through the application of directional filters to our raw magnetic data. Our interpretation of results images E-W and N-S to NW-SE strikes (e.g. Figure 11) as principal directions of the faults present in the area. These would be transtensive structures belonging respectively to the TMVB tectonics, extending to the north, and to the older B&R, ENE-directed extensive tectonics. We have also defined dimensions and depth of the magnetic body that we believe could be the heat source of the geothermal system in existence, described below.

1 GEOTHERMAL SYSTEM UNDER LAKE CUITZÉO

Thinned crust is often characterized by listric normal faults which tend to flatten at a depth proximal to the brittle-ductile transition (Jackson and McKenzie, 1983; Brogi *et al.*, 2003). The top of the reflective zone is generally located at about 15±5 km (McCarthy and Thompson, 1988; Mayer *et al.* 1997) but it tends to be shallower beneath regions with higher heat flow (Ranalli, 1995). An example can be found in southern Tuscany, central Italy, in the geothermal areas of Lardarello and Amiata (Batini *et al.*, 1978; 1983; Borgia *et al.*, 2014), where the regional average heat-flow is very high (120 mW/m2; Brogi *et al.*, 2003) and the brittle-ductile transition reach depths as shallow as 3-6 km (Batini *et al.*, 1985; Liotta and Ranalli, 1999), together with its shear-decollement zone properties (Borgia *et al.*, 2014; Mazzoldi *et al.*, 2015). At this depth main listric normal faults flatten.

Along the length of the E-W Chapala-Tula fault system – a proto-continental rift for some authors (see above) – the general northward extension, the frequency of geothermal areas, the high average heat flow (≥80 mW m^{-2}) and the average low dip of the domino fault-systems (lower than 70₀ between Morelia and lake Cuitzeo), make us suppose that the main E-W structures, coeval to the TMVB (8-10 Ma, and potentially already active during TMVB basement volcanism, >15 Ma, Mendoza-Ponce *et al.*, 2018), find a decollement shear-zone at a depth of no more than 8-10 km (probably shallower) – at which level they flatten. On the other hand, being active since the construction of the TMVB, NW- to N-trending Basin&Range faults, older than 20 Ma and with a higher angle of dip, could reach deeper than 15 km: the imposition of the regional average high heat-flow in the area, some 10 Ma (or 15-18 Ma, depending on whether the TMVB basement volcanism is considered as a main player for heat-flow and E-W faults activation), only relatively affected their geometry.

From these observations we derive our essential conceptual model of the geothermal system. In Figure 12a an idealized section cutting along the longitude of the TMVB is presented. The image summarizes the most recent models for the subduction of the Rivera and Cocos plates, previously described, with the two main gaps in Quaternary volcanism at the surface (Colima Gap and Tzitzio Gap) coinciding with the presence of tear faults at depth. This geometry involves a relatively strong vertical heat-flow for those sectors interested by the tears. Figure 12b depicts our conceptual model of the geothermal system. A soaring basaltic/andesitic magmatic body, exploiting a B&R structure of the T-VdS fault system for its rising, got trapped at near-surface level under a thick layer of plastic clay, identifiable with Cuitzeo lacustrine sedimentation, which interrupted its vertical motion, sometime during the last 500 ka. Hydrothermal calcite interesting B&R fault planes on the southern shore of the lake (figure 7d), and thick sinter deposits near hydrothermal springs, suggest that the system might have been bigger and more vigorous in the past. Activity of the N-S faults would have made it possible for a portion of the magma to reach the surface, through the clayey caprock, forming the andesitic island in the middle of the lake. Also, as shown by geological and geophysical analyses (e.g., figures 7a, 9b, 11), the whole peninsula of Cuitzeo may be related to this same intrusion through a E-W structure, more active than B&R, interesting the main part of its extension. Along the depth of the crystallized, still hot intrusion, water would heat up and consequently ascend to the surface, through listric E-W fault planes, more active and highly fractured (permeable) along their intersections with almost vertical B&R planes. These permeable intersections control the location of geothermal springs at the surface (e.g. Sibson, 1990; Figure 12b).

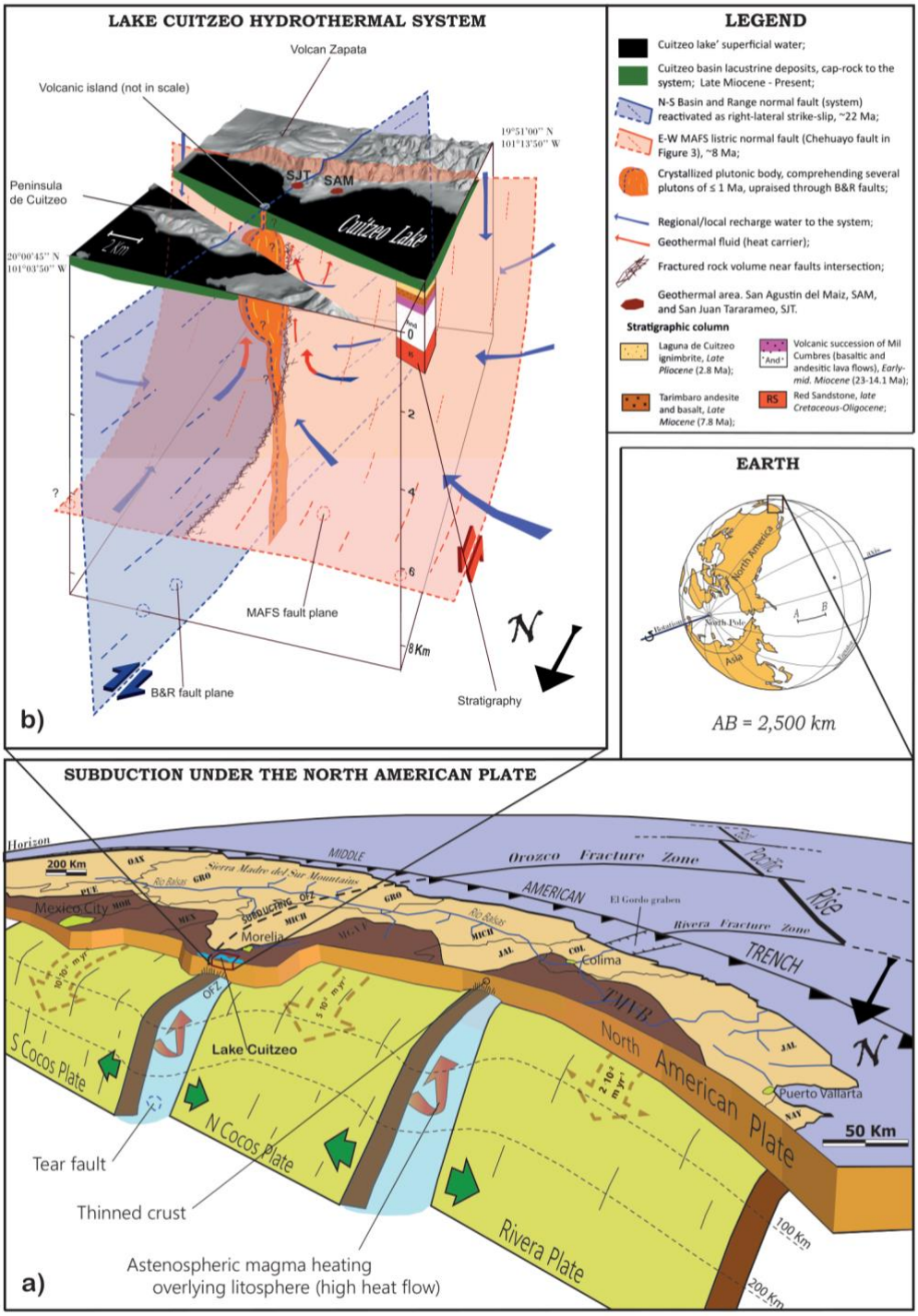

Figure 12. A) 3D representation of the subduction process under the North American Plate, as described in the text. The image highlights the importance of the subduction of fracture zones, the consequent presence of tear faults and their effect on surface volcanism (Tzitzio and Colima Gaps). While the dotted arrows over the subducting plate segments represent their (subduction) velocity, the red arrows drafted in correspondence with the tear faults separating plate' segments represent the toroidal flow of mantle around the Rivera and N Cocos plates (e.g., León-Soto *et al.*, 2009) and the resulting high heat-flow; B) 3D representation of our conceptual model of the geothermal system. Hot magma, ascending through a B&R fault found in a thick layer of lake sediments a barrier to reach the surface. A geothermal system is then created: hot water finds its way upward through fractured rocks near the intersection of B&R and TMVB faults.

At San Agustin del Mais, there is already some experience in geothermal development, thanks to different thermal resorts in the area, and geothermal fluid at about 130ºC is exploited at some 300 m depth (personal communication from spa owner). The estimated reservoir temperatures (150-220ºC, par. 2.4) and the mixing trend of the geothermal fluid (Segovia *et al.*, 2005) lead to the hypothesis that fluid at T>150ºC can be economically harvested somewhere around 500-600 m depth, provided the fractured zone of the main E-W fault bordering the southern bank of the Cuitzeo lake is targeted, particularly near its intersection with B&R structures, to avoid permeability issues during production. Geothermal exploitation at the site may be profitable to the industry and probably also to the local economy, although, on top of the presumed environmental stress delivered to an already polluted area, less heat may be available to local spas after beginning of production.

2 ALIGNMENTS OF CONES IN THE MGVF AND ORIGIN OF THE PLUME

Within MGVF authors have detected small-cones alignments following geologic lineaments, confirming that distribution of volcanoes can be the expression of stress conditions in the crust during activity (Hasenaka, 1984; Hasenaka and Carmichael, 1985; Cebriá *et al.*, 2010). In the southern half of the field, NE-striking alignments of cinder cones are evident (Ban *et al.*, 1992; Figure 13), coinciding with the orientation of the Tenochtitlán Fault System whose mean faults strike parallels the relative motion vector of the Cocos and North American plates (40º; DeMets *et al.*, 1990), defining an approximately NW-SE σ_3. These structures controlled the spatial distribution of many monogenetic and polygenetic volcanoes within the TMVB, hold evidences of Holocene reactivation, and disciplined the eruption of >70 cinder cones in MGVF, younger than 40,000yr (Ban *et al.*, 1992; Cebriá *et al.*, 2010; Figure 13). NE-striking lineaments contain Paricutin and Jorullo volcanoes (recently active) at their SW edges, and, if prolonged towards the NE, would interest our study area. Although results of our geophysical survey do not support the existence of NE-SW faults below Cuitzeo lake, these structures exist some km south of the SW shore of the lake (see Figures 2, 4, 7 and 13).

In the northeastern and northwestern parts of MGVF, authors described alignments of cinder cones with E-W strikes (Hasaka and Carmichael, 1985; Ban *et al.*, 1992), clearly related to the Chapala-Tula fault system. These faults, potentially delineating a young rift zone over the axis of TMVB, may also be invoked as cause for the ascent of the plume, below the lake, although their relatively low angle of dip would make this option less preferable.

The last lineament of interest is located at the northeastern sector of the MGVF, where some 13 maars (and many cinder-cones, not represented in figure 13), aged between 1.8 and 0.075 Ma (Aranda-Gomez and Carrasco-Nuñez, 2014) are distributed within an elongated 7 km by 50 km stripe, oriented NNW-SSE. This has been taken as evidence of a pre-existing buried fault system, a zone of deep crustal discontinuity enabling magmas to reach the surface (Murphy, 1982; Uribe-Cifuentes and Urrutia-Fucugauchi, 1999): ascending magma encountered the regional aquifer, favoring the generation of phreatomagmatic eruptions (Aranda-Gomez and Carrasco-Nuñez, 2014). Some of these maars hold lower crustal xenoliths, which is proof of their deep origins (Uribe-Cifuentes and Urrutia-Fucugauchi, 1999; Ortega-Gutiérrez *et al.*, 2014).

Following the most recent models (e.g. Blatter and Hammersley, 2010; Stubailo *et al.*, 2012), this zone of crustal weakness occupy part of the projection on the surface of the tear fault caused at depth by the subduction of the Orozco Fracture Zone (Figure 12a), which has a high heat

flow, favoring the ascent of astenospheric magma through the lower crust. Figure 13 highlights how, on a map, the alignment of maars strikes parallel to the continuation of the subducting OFZ and, on the ground, to the Tzitzio-Valle de Santiago fault system, already active during Basin & Range tectonics and still today.

We can further our hypothesis based on the volume of magnetic rock needed to create such an anomaly on the surface. If we assign to the magnetic source a diameter of say 3 km in 2D (Figure 9a and 10) and estimate for the plume a similar thickness (3 km, low appraisal), we would have a volume somehow higher than 20 km^3, higher than characteristic values of erupted material for monogenetic cinder cones (Max registered 5 km^3, Hasenaka and Carmichael, 1985), let alone maars volcanoes. Alaniz-Alvarez *et al.* (1998) observed how, over the TMVB, monogenetic small cones are preferentially oriented parallel to east-west normal faults with high slip rates; on the other hand, polygenetic volcanoes align along faults with low displacement rates (north-south B&R faults). The crystallized magmatic body under Cuitzeo lake, affected by different extensional tectonics, may be more relatable to a shield volcano of the MGVF and, in turn, might have enjoyed different recharge of magma, piling below the clay sediments, during its history.

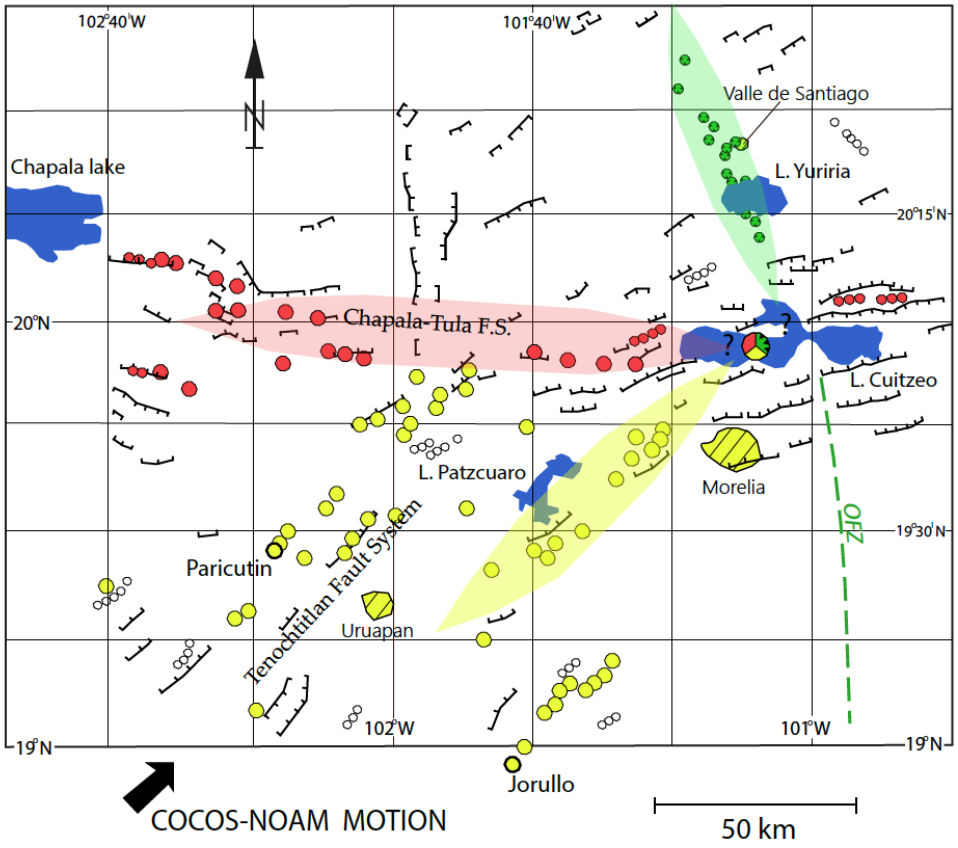

Figure 13. Represented on the map are alignments of volcanic edifice belonging to the MGVF. Particularly, in yellow are depicted some of the cinder cones following Tenochtitlán Fault System structures (N40o); in red, cinder cones are aligned with Chapala-Tula F.S. faults; in green, maars volcanoes are aligned along the Tzitzio-Valle de Santiago Fault System, as described in the text.

2.1 NEW RESULTS

In 2017 researchers from Universidad Michoacana de San Nicolas de Hidalgo (UMSNH) dated some of the E-W normal faults near Cuitzeo lake at about 18 Ma and the island in the middle of the lake (considered in this study) at 17 Ma, through $^{40}Ar/^{39}Ar$ analysis. As we detailed through the text, we believe this age for E-W faults of the Morelia-Acambay fault system reflects the imposition of an early TMVB-basement volcanism (and related heat-flow) which generated the right stress-field for the creation of these structures, probably with a pure extensional motion, during early Miocene times. This new insight might have scientists think again on the age of lake Cuitzeo, currently believed to be around 10 Ma, but probably older. The age of the island is another issue, having been related to the still-hot, crystallized, basic plume under the lake, in this work. An age of 17 Ma would not give any chance to a magmatic body to still be at an interesting temperature for feeding a hydrothermal system at present. A volume of magma as the one imaged in this work would cool down in no longer than say 500 ka after underground emplacement and we may fit this new finding (the age of the island) in our model in basically two ways. First, as we explained in the previous paragraph, the specific structural background of the study area (main N-S and E-W faults intersection) can influence the magma supply and provide recharge over time. Hence, while the island may be an early expression of the phenomenon, repeated magma top-ups from below might have influenced the strength of the geothermal system along time. In this case, a direct affinity with MGVF volcanism is less unambiguous. A second loophole in accounting for the age of the volcanic island is that it might not be related at all with the geothermal arrangement at the site. We believe new geophysical and geological studies should focus on the characterization of perspective geothermal sites laying along the TMVB, with the aim of easing future explorations and broadening general knowledge.

ACKNOWLEDGEMENTS

We feel particularly grateful to Dr. Cifuentes-Nava, Universidad Nacional Autonoma de Mexico, Instituto de Geophysica, Morelia, Mich., for allowing the usage of the Encom PA software and for sharing data from the magnetic station of Teoloyucán. We thank Dr. Lopez-Loera, Instituto Potosini de Investigaciòn Cientifica y Tecnologica, San Luis Potosí, San Luis Potosí, for suggestions about the field work. AM was funded by a studentship from CeMIE-Geo, Project 17, with funding from SENER-CONACYT, and feel thankful to INICIT-UMSNH for the usage of infrastructures.

REFERENCES

Aguirre-Díaz, G.J., and Labarthe-Hernandez, G., 2003. Fissure ignimbrites: Fissure-source origin for voluminous ignimbrites of the Sierra Madre Occidental and its relationship with Basin and Range faulting. Geology, 31, 773–776;

Alaniz-Alvarez, S.A., A.F. Nieto-Samaniego and L. Ferrari, 1998. Effects of strain rate in the distribution of monogenetic and polygenetic volcanism in the Trans-Mexican Volcanic Belt. Geology 26(7). DOI: 10.1130/0091-7613(1998)026<0591:EOSRIT>2.3.CO,2;

Alba-Aldarve, L. A., Reyes-Salas, M., Morán-Zenteno, D., Angeles-Garcia, S. y Corona-Esquivel R., 1996, Geoquímica de las rocas volcánicas terciarias de la región de Taxco-Huautla: Actas Instituto Nacional de Geoquímica, v. 2, p. 39–44;

Aranda-Gómez, J.J. and F. McDowell, 1998. Paleogene extension in the Southern Basin and Range province of Mexico: Syn-depositional tilting of Eocene Red Beds and Oligocene volcanic rocks in the Guanajuato mining district. Int. Geol. Rev,40(2), 116-134;

Aranda-Gomez, J.J. and G. Carrasco-Nuñez, 2014. The Valle de Santiago maars, México: the record of magma-water fluctuations during the formation of a basaltic maar (La Alberca) and active post-desiccation subsidence at the bottom of a maar lake (Rincón de Parangueo). Conf. Proc. 5th Int. Maar Conference. Nov. 20, 2014, Queretaro, Mexico;

Arredondo-Fragoso, J.J., 1983. Levantamiento gravimetrico en la zona central de la laguna de Cuitzeo, Michoacán. Informe 29-83, Comision Federal Electricidad, Gerencia de proyectos geotermicos. Mexico;

Ban, M., T. Hasenaka, H. Delgado-Granados and N. Takaoka, 1992. K-Ar ages of lavas from shield volcanoes in the Michoacán-Guanajuato volcanic field, Mexico. Geofisica Internacional 31, 4: 467-473;

Bandy, W.L., 1992. Geological and Geophysical Investigation of the Rivera-Cocos Plate Boundary: Implications for Plate Fragmentation. Ph.D. Dissertation, Texas A&M University, College Station, Texas, 195p;

Bandy W.L., Mortera-Gutierrez C., Urrutia-Fucugauchi J. and Hilde T.W.C., 1995. The subducted Rivera-Cocos plate boundary: Where is it, what is it, and what is its relationship to the Colima rift?. Geophys. Res.Lett., 22, 3075-3078;

Bandy W.L., T.W.C. Hilde and C.-Y. Yan, 2000. The Rivera-Cocos plate boundary: Implications for Rivera-Cocos relative motion and plate fragmentation, in Cenozoic Tectonics and Volcanism of Mexico, edited by H. Delgado-Granados, G. Aguirre-Díaz, and J.M. Stock, Spec. Pap. Geol. Soc. Am., 334, 1–28;

Baranov, V., 1957. A new method for interpretation of aeromagnetic maps: pseudo-gravity anomalies, Geophysics, 22, 359-383;

Batini, F., Burgassi, P.D., Cameli, G.M., Nicolich, R., Squarci, P., 1978. Contribution to the study of the deep lithospheric profiles: deep reflecting horizons in Larderello-Travale Geothermal field. Mem. Soc. Geol. Ital. 19, 477– 484;

Batini, F., Bertini, G., Giannelli, G., Pandeli, E., Purceddu, M., 1983. Deep structure of the Larderello geothermal field: contribution from recent geophysical and geological data. Mem. Soc. Geol. Ital. 5, 219– 235;

Batini, F., G. Bertini, G. Giannelli, E. Pandeli, E. Puxeddu and I. Villa, 1985. Deep structures, age and evolution of the Larderello-Travale geothermal field. Geothermal Res., Comm. Transaction, 9 (1978), 1-7;

Blatter, D., G. Farmer and I. Carmichael, 2007. A north-south transect across the central Mexican volcanic belt at 100oW: Spatial distribution, petrological, geochemical, and isotopic characteristics of quaternary volcanism, J. Petrol., 48, 901–950;

Blatter, D.L. and L. Hammersley, 2010. Impact of the Orozco Fracture Zone on the central TMVB. J. Volc. Geother. Res. 197 (2010) 67–84;

Borgia, A., Mazzoldi, A., Brunori, C.A., Allocca, C., Delcroix, C., Micheli, L., Vercellino, A., Grieco, G., 2014. Volcanic spreading forcing and feedback in geothermal reservoir development, Amiata volcano, Italia. J. Volcanol. Geotherm. Res. 284 (2014), 16;

Brogi, A., Lazzarotto, A., Liotta D. and G. Ranalli, 2003. Extensional shear zones as imaged by reflection seismic lines: the Lardarello geothermal field (central Italy). Tectonophysics 363 (2003), 127–139;

Campa-Uranga, M.F. and P.J. Coney, 1983. Tectono-stratigraphic terranes and mineral resource distribution in Mexico. Canadian Journal of Earth Sciences, 20, 623 1040-1051;

Campos-Enriquez, O.J., Herrera, M.C.R. and E. Bigurra-Pimental, 1988. Resultados preliminares del estudio magnetotelurico del área geotérmica de Araró y San Agustin del Maiz, Mich., MX. Informe 13/88. Comision Federal Electricidad, Gerencia de proyectos geotermicos. Mexico;

Cashman, P.H., J.E. Faulds and N.H. Hinz, 2012. Regional variations in structural controls on geothermal systems in the Great Basin. GRC Transactions, Vol. 36, 2012; 25-30;

Cebriá, J.M., C. Martin-Escorza, J. Lopez-Ruiz, D. Moran-Zenteno & B.M. Martiny, 2010. Numerical recognition of alignments in monogenetic volcanic areas: Example from the Michoacán-Guanajuato Volcanic Field in Mexico and Calatrava in Spain. J. Volc. Geoth. Res., 2010, 1-4;

Clemente-Chavez A., A. Figueroa-Soto, F.R. Zuñiga, M. Arroyo, M. Montiel and O. Chavez, 2013. Seismicity at the northeast edge of the Mexican Volcanic Belt (MVB) and activation of an undocumented fault: the Peñamiller earthquake sequence of 2010–2011, Querétaro, Mexico. Nat. Hazards Earth Syst. Sci., 13, 2521-2531;

Coolbaugh, M.F., Raines, G.L., Zehner, R.E., Shevenell, L., and Williams, C.F., 2006. Prediction and discovery of new geothermal resources in the Great Basin: Multiple evidence of a large undiscovered resource base: Geothermal Resources Council Transactions, v. 30, p. 867-873;

Cooper, G.R.J. and D.R. Cowan, 2004. Filtering using variable order vertical derivatives. Computer & Geoscience, 30, 455-459;

Cooper, G.R.J. and D.R. Cowan, 2008. Edge enhancement of potential-field data using normalized statistics. Geophysics, 73 (3), H1–H4;

Cordell, L. and Grauch, V.J.S., 1985. Mapping basement magnetization zones from aeromagnetic data in the San Juan Basin, New Mexico. In: The Utility of Regional Gravity and Magnetic Anomalies Maps. Society of Exploration Geophysicists, 181–197;

Curewitz, D. and J.A. Karson, 1997. Structural settings of hydrothermal outflow: Fracture permeability maintained by fault propagation and interaction. Journal of Vulcanology and Geothermal Research, 79. 149-168;

DeMets, C., R.G. Gordon, D.F. Argus and S. Stein, 1990. Current plate motions. Geophysical J. International, 101: 425-478;

Dickinson, W.R., and Lawton, T.F., 2001. Carboniferous to Cretaceous assembly and fragmentation of Mexico: Geological Society of America Bulletin, v. 113, p. 1142–1160, doi: 10.1130/0016-7606(2001)113<1142;

Dougherty S.L., Clayton R.W. and Helmberger D.V., 2012. Seismic structure in central Mexico: Implications for fragmentation of the subducted Cocos plate. J. Geophys. Res. 117;

Ego F. and V. Ansan, 2002. Why is the Central Trans-Mexican Volcanic Belt (102o-99oW) in transtensive deformation? Tectonophysics 359, 189-208;

Faulds, J.E., Coolbaugh, M., Bouchot, V., Moek, I., Oguz. K., 2010. Characterizing

Structural Controls of Geothermal Reservoirs in the Great Basin, USA, and Western Turkey:Developing Successful Exploration Strategies in Extended Terranes. International Geothermal Association. World Geothermal Congress 2010, Apr 2010, France. 11 p. <hal-00495884>;

Faulds, J.E., Hinz, N., Kreemer, C. and M. Coolbaugh, 2012. Regional Patterns of Geothermal Activity in the Great Basin Region, Western USA: Correlation with Strain Rates. GRC Transactions, 36;

Faulds, J.E. and N. Hinz, 2015. Favorable Tectonic and Structural Settings of Geothermal Systems in the Great Basin Region, Western USA: Proxies for Discovering Blind Geothermal Systems. Proceedings of the World Geothermal Congress 2015. Melbourne, Australia, 19-25 April 2015;

Fedi, M. and G. Florio, 2001. Detection of potential field source boundaries by enhanced horizontal derivative method. Geophysical Prospecting, 49, 40-58;

Ferrari, L., Garduño, V.H., Pasquare` G., and Tibaldi, A., 1991, Geology of Los Azufres caldera, Mexico, and its relationships with regional tectonics: J. Volc. Geoth. Res., 47, 129–148;

Ferrari, L., Pasquaré, G., Venegas, S., Castillo, D. and F. Romero, 1994. Regional tectonics of western Mexico and its implications for the northern boundary of the Jalisco block. Geofis. Int. 33, 139-151;

Ferrari, L., Lopez-Martinez, M., Aguirre-Dıaz, G. and G. Carrasco-Nuñez, 1999. Space–time patterns of Cenozoic arc volcanism in central Mexico: from the Sierra Madre Occidental to the Mexican Volcanic Belt. Geology 27, 303–306;

Ferrari, L., G. Pasquare´, S. Venegas-Salgado, and F. Romero-Rios, 2000. Geology of the western Mexican Volcanic Belt and adjacent Sierra Madre Occidental and Jalisco block, Geol. Soc. Am. Spec. Pap., 334, 65–84, 2000;

Ferrari, L., and Rosas-Elguera, J., 2000. Late Miocene to Quaternary extension at the northern boundary of the Jalisco block, western Mexico: The Tepic-Zacoalco rift revised, in Delgado-Granados, H., *et al.*, eds., Cenozoic tectonics and volcanism of Mexico: Geological Society of America Special Paper 334, 41–63;

Ferrari, L., López-Martínez, M., and Rosas-Elguera, J., 2002. Ignimbrite flare-up and deformation in the southern Sierra Madre Occidental, western Mexico—implications for the late subduction history of the Farallon Plate: Tectonics, 21, doi:10.1029/2001TC001302;

Ferrari, L., Valencia-Moreno M and S. Bryan, 2007. Magmatism and tectonics of the Sierra Madre Occidental and its relation with the evolution of the western margin of North America. in Alaniz-Álvarez, S.A., and Nieto-Samaniego, Á.F., eds., Geology of México: Celebrating the Centenary of the Geological Society of México: Geological Society of America. Special Paper 422, p. 1–39, doi: 10.1130/2007.2422(01);

Ferrari, L., T. Orozco-Esquivel, V. Menea, M. Menea, 2012. The dynamic history of the Trans-Mexican Volcanic Belt and the Mexico subduction zone. Tectonophysics 522-523 (2012), 122-149;

Ferreira, F.J.F., de Castro, L.G., A.B.S. Bangiolo, J. deSouza and M.A.T. Romeiro, 2011. Enhancement of the total horizontal gradient of magnetic anomalies using tilt derivatives: Part II – Application to real data. 81st Annual International Meeting, SEG, Expanded Abstract, 887-891;

Ferreira, F.J.F., Souza, J., Bongiolo, A.B.S. and L.G. de Castro, 2013. Enhancement of the total horizontal gradient of magnetic anomalies using the tilt angle. Geophysics, 78, (3). J33-J41;

Fournier, R. O. and Rowe, J.J., 1966. Estimation of underground temperatures from the silica content of water from hot springs and wet-steam wells. Am. J. Sci., 264: 685–697;

García-Palomo, A., J.L. Macias and V.H. Garduño-Monroy, 2000. Miocene to Recent structural evolution of the Nevado de Toluca volcano region, central Mexico. Tectonophysics, 318, 281-302;

Garduño-Monroy V.H. and N.A. Gutiérrez-Negrín, 1992. Magmatismo, hiatus y tectónismo de la Sierra Madre Occidental y del Cinturón Volcánico Mexicano. Geofísica Internacionál 31, 417-429;

Garduño-Monroy V.H., Spinner J., Ceragioli E., 1993. Geological and structural study of the Chapala rift, State of Jalisco, Mexico. Geofís. Int. 32(1993), 487-499;

Garduño-Monroy V.H., R. Pérez-Lopez, I. Israde-Alcantara, M.A. Rodríguez-Pascua, E. Szynkaruk, V.M. Hernández-Madrigal, M.L. García-Zepeda, P. Corona-Chávez, M. Ostroumov, V.H. Medina-Vega, G. García-Estrada, O. Carranza, E. Lopez-Granados and J. C. Mora Chaparro, 2009. Paleoseismology of the southern Morelia-Acambay fault system, central Mexico. Geofis. Int., 48 (3), 319-335;

Gianiyu, S.A., Badmus, B.S., Awoyemi, M.O., Akinyemi, O.D. and Olurin O.T., 2013. Upward Continuation and Reduction to Pole Process on Aeromagnetic Data of Ibadan Area, South-Western Nigeria. Earth Science Research, 2, 1, 66-73;

Glen J.M.G., Egger, A.E. and D.A. Ponce, 2008. Structures controlling geothermal circulation identified through gravity and magnetic transects, Surprise Valley, California, NW Great Basin. GRC Transactions, 32, 2008, 279-283;

Glen J.M.G., Egger, A.E., Ippolito C., Athens N., 2013. Correlation of geothermal springs with sub-surface fault terminations revealed by high-resolution, UAV-Acquired magnetic data. Proceedings of the Thirty-eight workshop on geothermal reservoir engineering. Stanford University, Stanford, California, February 11-13 2013, SGP-TR-198;

Goldstein, B., G. Hiriart, R. Bertani, C. Bromley, L. Gutiérrez-Negrín, E. Huenges, H. Muraoka, A. Ragnarsson, J. Tester, V. Zui, 2011. Geothermal Energy. In IPCC Special Report on Renewable Energy Sources and Climate Change Mitigation [O. Edenhofer, R. Pichs-Madruga, Y. Sokona, K. Seyboth, P. Matschoss, S. Kadner, T. Zwickel, P. Eickemeier, G. Hansen, S. Schlömer, C. von Stechow (eds)], Cambridge University Press, Cambridge, United Kingdom and New York, NY, USA;

Gómez-Vasconcelos, M.G., Garduño-Monroy, V.H., Macías, J.L., Layer, P.W. and Benowitz, J.A., 2015. The Sierra de Mil Cumbres, Michoacán, México: Transitional volcanism between the Sierra Madre Occidental and the Trans-Mexican Volcanic Belt. Journal of Volcanology and Geothermal Research, 301, 128-147;

Grauch .J.S. and Cordell L., 1987. Limitations of determining density or magnetic boundaries from the horizontal gradient of gravity or pseudogravity data. Geophysics, vol. 52, 1; 118-121;

Gutiérrez-Negrín, L., 1988. The La Primavera (Jalisco, Mexico) Geothermal Field. Geothermal Resources Council, TRANSACTIONS, Vol. 12, 1988 - http://pubs.geothermal-library.org/lib/grc/1001702.pdf;

Hasenaka, T., M. Ban and H.D. Granados, 1994. Contrasting volcanism in the Michoacán-Guanajuato Volcanic Field, central Mexico: Shield volcanoes vs. cinder cones. Geofísica Internacional, 33 (1). 125-138;

Hasenaka, T., 1994. Size, distribution and magma output rate for shield volcanoes of the Michoacán-Guanajuato Volcanic Field, central Mexico. J. Volc. Geoth. Res., 63(1-2): 13-31;

Hasenaka, T. and Carmichael, I.S.E., 1985. The cinder cones of Michoacán-Guanajuato, central Mexico: their age, volume, distribution, and magma discharge rate, J. Volc. Geoth. Res., 25, 104-124;

Hasenaka, T. and Carmichael, I.S.E., 1987. The cinder cones of Michoacán-Guanajuato, central Mexico: Petrology and chemistry. J. Petrology, 28(2): 241-269;

Henry, C.D. and J.J. Aranda-Gomez, 1992. The real southern Basin and Range: Mid- to late Cenozoic extension in Mexico. Geology, 20, p. 701-704;

Hood, P.J., 1965. Gradient measurements in aeromagnetic surveying. Geophysics, 30, 891-902;

Huppert, H. E., and R. S. J. Sparks, 1988. The generation of granitic magmas by intrusion of basalt into continental crust. J. Petrol., 29, 599 – 642;

International Finance Corporation, 2013. Success of Geothermal Wells: a Global Study. Prepared by International Finance Corporation and GeothermEx, Inc. http://www.ifc.org/wps/wcm/connect/7e5eb4804fe24994b118ff23ff966f85/ifc-drilling-success-report-final.pdf?MOD=AJPERES;

Jackson, J. and D. McKenzie, 1983. The geometrical evolution of normal fault systems. J. Structural Geology, 5, 5, 471-482;

Jackson M. and J.A. Bowies, 2014. Curie temperatures of titanomagnetite in ignimbrites: Effects of emplacement temperatures, cooling rates, exsolution, and cation ordering. Geochemistry, Geophysics, Geosystems, (15), 11. 4343-4368;

Keating, P.B: and M. Pilkington, 1990. An automated method for the interpretation of magnetic vertical-gradient anomalies. Geophysics, 55, 336-343;

Kipsang, C., 2015. Cost model for geothermal wells. Proceedings of the World Geothermal Congress 2015. Melbourne, Australia, 19-25 April 2015;

Langridge, R.M., Weldon, R.J.II, Moya, J.C., and Suárez, G., 2000. Paleoseismology of the 1912 Acambay earthquake and the Acambay-Tixmadeje´ fault, Trans-Mexican Volcanic Belt: Geophys. Res., 105, 3019–3037;

León-Soto, G., Ni, J.F., Grand, S.P., Sandvol, E., Valenzuela, R.W., Speziale, M.G., González, J.M.G., Reyes, T.D., 2009. Mantle flow in the Rivera–Cocos subduction zone. Geophysical Journal International 179, 1004–1012;

Liotta, D. and G. Ranalli, 1999. Correlation between seismic reflectivity and rheology in extended lithosphere: southern Tuscany, Inner Northern Apennines, Italy. Tectonophysics 315, 109–122;

Lopez-Loera, H., Urrutia-Fucugauchi and L.M. Alva-Valdidia, 2010. Magnetic characteristics of fracture structure of the Colima Volcanic Complex, western Mexico. Geosphere, 6(1), 35-46;

Luhr, J.F.S., A. Nelson, J.F. Allen and I.S.E. Carmichael, 1985. Active rifting in southwestern Mexico: manifestations of an incipient eastward spreading ridge jump. Geology, 13, 54-57;

Manea, V.C., Manea, M., Kostoglodov, V., Sewell, G., 2005. Thermo-mechanical model of the mantle wedge in central Mexican subduction zone and a blob tracing approach for the magma transport. Physics of the Earth and Planetary Interiors 149, 165-186;

Márquez, A., R. Oyarzun, M. Doblas, and S. P. Verma, 1999. Alkalic (ocean-island basalt type) and calc-alkalic volcanism in the Mexican Volcanic Belt: a case for plume-related magmatism and propagating rifting at an active margin? Geology, 27, pp. 51-54;

Mayer, G., Mai, P.M., Plenefisch, T., Echtler, H., Lu Schen, E., Wehrle, V., Muller, B., Bonjer, K.P., Prodehl, C., Fuchs, K., 1997. The deep crust of the Southern Rhine Graben: reflectivity and seismicity as images of dynamic processes. Tectonophysics 275, 15-40;

Mazzoldi, A., Borgia, A., Ripepe, M., Marchetti, E., Ulivieri, G., Della Schiava, M. and C. Allocca, 2015. Faults strengthening and seismicity induced by geothermal exploitation of a spreading volcano, Mt. Amiata, Italia. J. Volc. Geoth. Res., 301(2015), 159-168;

Mazzoldi, A., J.A. Guevara-Alday, J.J. Gomes-Cortes and V.H. Garduño-Monroy, 2016. Papel de estructuras Basin and Range en la formación del sistema geotérmico al centro-sur del lago Cuitzeo, segmento central del Cinturòn Volcanico Mexicano. Asociación Geotérmica Mexicana. Memorias de XXIII Congreso Anual - Morelia, Mich., 10-11 Marzo 2016;

McCann, W.R. and Habermann, R.E., 1989. Effects of the subduction of bathymetric highs. Pure and Applied Geophysics 129 (1/2), 41-69;

McCarthy, J. and Thompson, G.A., 1988. Seismic imaging of extended crust with emphasis on the western United States. Geol. Soc. Am. Bull. 100, 1361-1374;

Mendoza-Ponce, A., Figueroa-Soto, A., Soria-Caballero, D. and V.H. Garduño-Monroy, 2018. Active faults sources for the Patzcuaro-Acambay fault system (Mexico): fractal analysis of slip rates and magnitudes Mw estimated from fault length. Nat. Hazards Earth Syst. Sci., 18, 3121-3135;

Miller, H. G., and V. Singh, 1994. Potential field tilt - A new concept for location of potential field sources. Applied Geophysics, 32, 213–217;

Morán-Zenteno, D. J., Alba-Aldave, L., Corona-Ezquivel, R., Reyes-Salas, M., Martínez-Serrano, R., and Angeles-García, S., 1999. Stratigraphy and tectonic significance of the Tertiary silicic volcanism in northern Guerrero, México: Revista Mexicana de Ciencias Geologicas, 15(2);

Murphy, G.P., 1982. The chronology, pyroclastic stratigraphy and petrology of the Valle de Santiago maar field, central Mexico. M.Sc. Thesis, University of California, Berkeley, USA;

Nabighian, M.N., 1972. The analytic signal of two-dimensional magnetic bodies with polygonal cross-section: Its properties and use for automated anomaly interpretation. Geophysics, 37: 507-517;

Nabighian, M.N., 1974. Additional comments on the analytic signal of two dimensional magnetic bodies with polygonal cross-section. Geophysics, 39, 85-92;

Nieto-Samaniego, A.F., Ferrari, L., Alvaniz-Alvarez, S.A., Labarthe-Hernandez, G. and R. Rosas-Elguera, 1999. Variation of Cenozoic extensión and volcanism accross the southern Sierra Madre Occidental volcanic province, Mexico. Geol. Soc. Am. Bull., 111, 347-363;

Nixon, G.T., 1982. The relationship between Quaternary volcanism in central Mexico and the seismicity and structure of subducted ocean lithosphere. Geol.Soc.Am.Bull., 93(6), 514-523;

Ortega-Gutiérrez, F., A. Gomez-Tuena, M. Elias-Herrera, L.A. Solari, M. Reyes-Salas and C. Masias-Romo, 2014. Petrology and geochemistry of the Valle de Santiago lower-crust xenoliths: Young tectonothermal processes beneath the central TMVB. Lithosphere, 6(5): 335-360;

Pardo, M. and G. Suárez, 1995. Shape of the subducted Rivera and Cocos plate in southern Mexico: seismic and tectonic implications. Journal of Geophysical Research 100, 12: 357-373;

Parsons, T.E., 1995. The Basin and Range province: Chapter 7. In: Continental Rifts: Evolution, Structure, Tectonics. USGS Pubblication, Edited by: Elsevier, Series number: 264. Pp. 277-324;

Pasquaré, G., Garduño-Monroy, V.H., Tibaldi, A. and M. Ferrari, 1988. Stress pattern evolution in the central sector of the Mexican Volcanic Belt. Tectonophysics, 146, 353-364;

Pasquaré, G., L. Ferrari, V. H. Garduño-Monroy, A. Tibaldi, and L. Vezzoli, 1991. Geological map of the central sector of Mexican Volcanic Belt, States of Guanajuato and Michoacán, Geol. Soc. Am. Map Chart Ser., MCH 072, 1 sheet, 20 pp., Geol. Soc. of Am., Boulder, Colo., 1991;

Pérez-Lòpez, R., D. Legrand, V.H. Garduño-Monroy, M.A. Rodriguez-Pascua, J.L. Giner-Robles, 2011. Scaling lwas of the size-distribution of monogenetic volcqnoes within the MGVF, Mexico. J. Volc. Geoth, Res. 201, 65-72;

Pipan, M., Forte, E., Del Ben, A., Nava-Alonzo, H.F., Giudetti G. and S. Supriyanto, 2010. Seismic and elettromagnetic study of reservoir properties for geotermal application. Proc. World. Geoth. Congr., 2010. Bali, Indonesia, April 2010;

Prol, R.M., 1991. Terrestrial heat flow in Mexico, in Exploration of the Deep Continental Crust; Terrestrial Heat Flow and the Lithosphere structure. Edited by V. Cermak and L. Rybach, 475-485. Springer-Verlag, New York, 1991;

Ranalli, G., 1995. Rheology of the Earth, 2nd ed. Chapman and Hall, London;

Ravat, D., Kirkham, K. and T.G. Hildenbrand, 2002. A source-depth separation filter: Using the Euler method on the derivatives of total intensity magnetic anomaly data. The leading edge. April 2002, 360-365;

Robelledo-Vieyra, M., Urrutia-Fucugauchi, J., Lopoez-Loera, H., 2010. Aeromagnetic anomalies and structural model of the Chicxulub multiring impact cráter, Yucatan, Mexico. Revista Mexicana de Ciencias Geologicas, 27, 1, 185-195;

Roest, W.R., Verhoef, J., Pilkington, M., 1992. Magnetic interpretation using 3-D analytic signal. Geophysics 57, 116-125;

Rosas-Elguera, J., L. Ferrari, Lopez-Martinez, M. and F.J. Urrutia.Fucugauchi, 1997. Stratigraphy and tectonics of the Guadalajara región and the triple junction area, western Mexico. Int. Geology Review, 39. 125-140;

Rowland, J.V. and R.H. Sibson, 2004. Structural controls on hydrothermal flow in a segmented system, Taupo Volcanic Zone, New Zeland. Geofluids 4, 259-283;

Salem, A., Williams S., Fairhead J.D., Ravat D. and Smith R., 2007. Tilt-depth method: A simple depth estimation method using first-order magnetic derivatives. The leading edge, December 2007, 1502-1505;

Segovia, N., Barragan, R.M., Tello, E., Alfaro, R., Mena, M., 2005. Geochemical exploration at Cuitzeo Basin Geothermal Zone (Mexico). J. Applied Science 5 (9), 1658-1664;

Servicio Geológico Mexicano, 1988. "Datos magnéticos (vuelos sistemáticos). Grid con datos cada 200 m: E14-A13 (Cuitzeo); E14-A14 (Zinapécuaro); F14-C83 (Moroleón); F14-C84 (Acámbaro)". Escala 1:50000. SGM. México, DF;

Sibson, R.H., 1981. Controls on low-stress hydro-fracture dilatancy in thrust, wrench and normal fault terrain. Nature 289, 665-667;

Sibson, R.H., 1990. Conditions for fault-valve behavior. Geological Society, London. Special Pubblication 54, 15-28;

Singh, S.K., Pardo, M., 1993. Geometry of the Benioff zone and state of stress in the overriding plate in central Mexico. Geophys. Res. Lett. 20, 1483 – 1486;

Stubailo, I., Beghein, C. and P.M. Davis, 2012. Structure and anisotropy of the Mexico subduction zone based on Rayleigh-wave analysis and implications for the geometry of the Trans-Mexican Volcanic Belt. J. Geoph. Res., 117. B05303;

Subir, K.S. and J.W. Morrow, 2011. An investigation of drilling success in Geothermal Exploration, Development and Operation. GRC Transaction, 35;

Suter, M., 1991. State of stress and active deformation in Mexico and the western Central America. In Slemmons, Engdahl, Zoback and Blackwell eds., Neotectonics of North America. Boulder, CO. Geological Society of America Decade Map Volume, 401-421;

Suter, M., Quintero-Leogorrote, O. and M. Lopez-Martinez, 1995a. The Acambay graben: active intra-arc extensión in the Trans-Mexican Volcanic Belt. Tectonics, 14, 1245-1262;

Suter, M., Carrillo-Martinez M., Lopez-Martinez, M. and E. Farrar, 1995b. The Aljibes half-graben—Active extensión at the boundary between the trans-Mexican volcanic belt and the Basin and Range Province, Mexico. Bull. Geol. Soc. Am. 107(6), 627-641;

Suter, M., Carrillo-Martınez, M. and O. Quintero-Legorreta, 1996. Macroseismic study of shallow earthquakes in the central and eastern parts of the Trans-Mexican volcanic belt. Bull. Seismol. Soc. Am. 86, 1952–1963;

Suter, M., J. Contreras, A. Gomez-Tuena, C. Siebe, O. Quintero-Lagorreta, A. Garcia-Palomo, J. Macias, S.A. Alaniz-Alvarez, A.F. Nieto-Samaniego and L. Ferrari, 1999. Effects of strain rate in the distribution of monogenetic and polygenetic volcanism in the Trans-Mexican Volcanic Belt. Geology 27(6): 571-575;

Suter, M., Lopez-Martınez, M., Quintero- Leogorrote, O., and M. Carrillo-Martınez, 2001. Quaternary intra-arc extension in the Central TMVB. Bull. Geol. Soc. Am. 113, 693– 703;

Thebault, E., Finlay, C., Beggan, C., Alken, P., Aubert, J., Barrois, O., Bertrand, F., Bondar, T., Boness, A., Brocco, L., Canet, E., Chambodut, A., Chulliat, A., Coisson, P., Civet, F., Du, A., Fournier, A., Fratter, I., Gillet, N., Hamilton, B., Hamoudi, M., Hulot, G., Jager, T., Korte, M., Kuang, W., Lalanne, X., Langlais, B., Leger, J.M., Lesur, V. and F. Lowes., 2015. International Geomagnetic Reference Field: the 12th generation. Earth, Planets and Space, 67:79;

Uribe-Cifuentes, R.M. and J. Urrutia-Fucugauchi, 1999. Paleomagnetic study of the Valle de Santiago volcanics, Michoacan-Guanajuato volcanic field, Mexico. Geofisica Internacional, Vol, 38. 4: 2017-230;

Urrutia-Fucugauchi, F.J. and J.H. Flores Ruiz, 1996. Bouguer gravity anomaly and regional crustal structure in central Mexico. Int. Geol. Rev. 38, 176–194;

Verduzco, B., J. D. Fairhead, C. M. Green, and C. MacKenzie, 2004. New insights into magnetic derivatives for structural mapping. The Leading Edge, 23, 116–11;

Venegas, S., F. Maciel and J.J. Herrera, 1985. Recursos geotérmico de la Faja Volcánica Mexicana. Geofis. Int., 24-1, 47-81;

Verma P.S. and T. Hasenaka, 2004. Sr, Nd and Pb isotopic and trace element geochemical constraints for a veined-mantle source of magmas in the MGVF, west-central Mexican Volcanic Belt. Geochemical J., 38, 43-65;

Verma, S.P., 2009. Continental Rift Setting for the Central Part of the Mexican Volcanic Belt: A Statistical Approach. The Open Geology J., 3, 8-29;

Wahyudi E.J., Kynantoro Y. and S. Alawiyah, 2017. Second vertical derivative using gravity data for fault structure interpretation. Int. Conf. on Energy Sc.(ICES 2016). doi :10.1088/1742-6596/877/1/012039;

Williams, H., 1950. Volcanoes of the Paricutin region. U.S.G.S. Bulletin 965-C: 281-353;

Zuñiga F.R., J.F. Pacheco, M. Guzman-Speziale, G.J. Aguirre-Díaz, V.H. Espíndola, E. Nava, 2003. The Sanfandila earthquake sequence of 1998, Queretaro, Mexico: activation of an undocumented fault in the northern edge of central Trans-Mexican Volcanic Belt. Tectonophysics 361, 229-238.